RAC1 in keratinocytes regulates crosstalk to immune cells by Arp2/3-dependent control of STAT1

Esben Pedersen[1], Zhipeng Wang[1], Alanna Stanley[2], Karine Peyrollier[1], Lennart M. Rösner[3], Thomas Werfel[3], Fabio Quondamatteo[2] and Cord Brakebusch[1,*]

[1]Biomedical Institute, BRIC, University of Copenhagen, Ole Maaløes Vej 5, 2200 Copenhagen, Denmark
[2]Anatomy Unit, NUI Galway, University Road, Galway, Ireland
[3]Department of Dermatology and Allergology, Hannover Medical School, Hannover, Germany
*Author for correspondence (cord.brakebusch@bric.ku.dk)

Accepted 6 August 2012
Journal of Cell Science 125, 5379–5390

doi: 10.1242/jcs.107011

Summary

Crosstalk between keratinocytes and immune cells is crucial for the immunological barrier function of the skin, and aberrant crosstalk contributes to inflammatory skin diseases. Using mice with a keratinocyte-restricted deletion of the *RAC1* gene we found that RAC1 in keratinocytes plays an important role in modulating the interferon (IFN) response in skin. These *RAC1* mutant mice showed increased sensitivity in an irritant contact dermatitis model, abnormal keratinocyte differentiation, and increased expression of immune response genes including the IFN signal transducer STAT1. Loss of *RAC1* in keratinocytes decreased actin polymerization *in vivo* and *in vitro* and caused Arp2/3-dependent expression of *STAT1*, increased interferon sensitivity and upregulation of aberrant keratinocyte differentiation markers. This can be inhibited by the AP-1 inhibitor tanshinone IIA. Loss of *RAC1* makes keratinocytes hypersensitive to inflammatory stimuli both *in vitro* and *in vivo*, suggesting a major role for *RAC1* in regulating the crosstalk between the epidermis and the immune system.

Key words: RAC1, Skin inflammation, STAT1

Introduction

Collaboration and crosstalk between keratinocytes and resident immune cells is considered to be crucial for the skin function as an immunological barrier and impaired crosstalk is believed to contribute to many if not all inflammatory skin diseases. The complex relationship between keratinocytes and immune cells makes it difficult to understand the etiology of chronic skin inflammations (Lowes et al., 2007; Wagner et al., 2010): do defects in keratinocyte barrier function or cytokine production by keratinocytes trigger activation of the immune system or is an abnormally activated immune system causing barrier defects and an altered cytokine profile of the keratinocytes?

RAC1 is a member of the Rho family of small GTPases, which controls various cellular processes such as ERK and AKT activity, actin polymerization, and ROS production (Bustelo et al., 2007). Previously, we and others showed that keratinocyte-restricted loss of *RAC1* results in normal development and maintenance of the interfollicular epidermis, but loss of hair follicles and defective wound healing (Chrostek et al., 2006; Tscharntke et al., 2007; Castilho et al., 2007; Castilho et al., 2010). We report now that decreased Arp2/3 dependent actin polymerization in *RAC1*-null keratinocytes induces the IFN-γ activated transcription factor STAT1, sensitizes *RAC1*-null keratinocytes towards IFN-γ produced by immune cells, and induces aberrant keratinocyte differentiation.

These data reveal a novel role for RAC1 and actin polymerization in skin immunity by regulating the innate immune response in keratinocytes, thereby affecting the crosstalk between keratinocytes and immune cells.

Results

RAC1 in keratinocytes controls sensitivity to skin inflammation

Mice with a keratinocyte-restricted deletion of the *RAC1* gene are resistant towards 7.12-dimethylbenz(a)anthracene/12-O-tetradodecanoyl-phorbol-13-acetate (DMBA/TPA) induced hyperproliferation and tumor formation in skin (Wang et al., 2010). Since DMBA/TPA induced skin tumors are dependent on a strong inflammatory response, we tested during our investigation, whether loss of *RAC1* decreases TPA-induced inflammation. Surprisingly, microarray gene expression analysis of epidermal cells from TPA treated *RAC1* ko and control mice revealed rather an increased inflammatory reaction in *RAC1*-null epidermis. Functional grouping of the genes upregulated more than twofold, using the DAVID program, revealed a significant enrichment of genes related to cytokines and inflammation, which included *IL-6* (4 fold), *CXCL10* (3.3 fold), *CXCL1* (2.4 fold), *TNFSF9* (2.3 fold) and *CCL2* (2.1 fold) (Fig. 1A). This increased inflammatory response was not due to an increased activation of classical NF-κB signaling, as nuclear phosphorylation of NF-κB at S536 was unchanged between control and *RAC1* ko epidermis treated or untreated with DMBA/TPA (supplementary material Fig. S1).

These data indicate that the TPA-induced skin inflammation does not require RAC1 function in keratinocytes, in contrast to TPA-induced hyperproliferation. They furthermore suggest that loss of *RAC1* in keratinocytes might promote skin inflammation.

To directly address this question, we applied a contact dermatitis model, where the ears of the mice are painted with croton oil, a TPA containing irritant. Indeed, mice lacking *RAC1* in keratinocytes showed a 3-fold increase in granulocyte

A

Pathway	N	P value	Fold
NOD-like receptor signaling pathway	5	2.10E-04	16
Developmental growth	5	7.60E-04	11.9
Cytokine	7	3.40E-05	11.2
Cytokine activity	7	5.50E-05	10.1
Growth	5	8.20E-03	6.2
Protein dimerization activity	8	2.60E-04	6.1
Positive regulation of transcription from RNA polymerase II promoter	9	1.00E-04	6
Positive regulation of cell proliferation	7	1.10E-03	5.9
Inflammatory response	5	1.40E-02	5.3
Positive regulation of transcription, DNA-dependent	9	2.80E-04	5.2

B

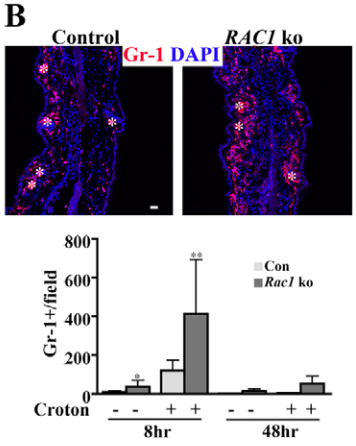

C

Pathway	N	P-Value	Fold
Small proline-rich	12	8.40E-16	42.9
Epidermis development	16	1.50E-11	10.9
Ectoderm development	16	3.70E-11	10.3
Cytokine	14	3.60E-08	7.7
Epithelial cell differentiation	11	1.70E-06	7.6
Cytokine activity	13	2.60E-06	5.7
Fatty acid metabolic process	10	3.00E-04	4.6
Cytokine-cytokine receptor interaction	11	3.70E-04	3.9
Inflammatory response	10	1.30E-03	3.8
Epithelium development	12	3.30E-04	3.8
Immune response	20	2.30E-06	3.6

D

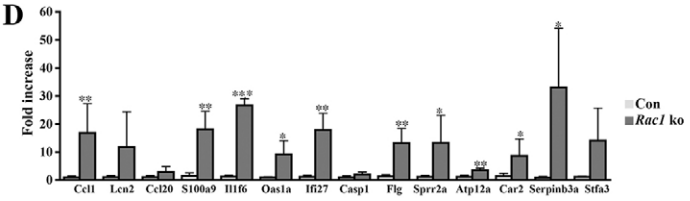

Fig. 1. Increased inflammatory response in TPA and croton oil treated *RAC1* ko skin. (**A**) Functional grouping of 83 genes increased more than twofold in *RAC1* ko epidermis treated for 2 w with TPA compared with TPA treated epidermis of control mice using the DAVID program. Gene groups related to inflammation are indicated in bold italics. "N" indicates the number of genes in the group. "Fold" indicates the fold enrichment of the group compared with a similar number of random genes (n=2/2). (**B**) Croton oil induced irritant dermatitis. Top, representative images of ears from control and *RAC1* ko mice stimulated with croton oil for 8 h stained for granulocytes (Gr-1) and nuclei (DAPI). Asterisks mark non-specifically stained sebaceous glands (scale bar, 20 μm). Bottom, quantification of Gr-1+ cells per field after 8 h and 48 h (three images per ear; n=12/12; *P<0.05, **P<0.001). (**C**) Functional grouping of 231 genes increased more than twofold in the epidermis of at least 3 out of 4 adult *RAC1* ko mice compared with control mice using the DAVID program. Bold indicates gene groups related to keratinocyte differentiation. Gene groups related to inflammation are indicated with bold italics. 'N' indicates the number of genes in the group. 'Fold' indicates the fold enrichment of the group compared with a similar number of random genes (n=4/4). (**D**) Gene expression analysis by qRT-PCR in epidermis of control and *RAC1* ko mice of 14 genes identified by microarray as upregulated in *RAC1* ko mice (n=4/4; *P<0.05, **P<0.001, ***P<0.0001).

infiltration after 8 h, which resolved after 48 h (Fig. 1B). Even in response to vehicle, *RAC1* mutant mice showed an increased granulocyte infiltration, confirming an increased sensitivity of *RAC1*-null skin towards inflammation.

Altered differentiation and increased expression of immune response related genes in *RAC1*-null epidermis

To understand the molecular reason underlying the increased inflammation in mice lacking *RAC1* in keratinocytes, we performed a gene expression analysis of epidermis of adult control and *RAC1* mutant mice. We identified 231 genes upregulated at least 2-fold in *RAC1*-null epidermis, excluding lowly expressed genes (basal expression level in *RAC1*-null below 100). Analyzing these genes by DAVID we found an enrichment of genes related to keratinocyte differentiation and inflammation, including many genes related to interferon response (*CXCL10, OAS1D, OAS1A, OAS1E, OAS2, OASL2, ISG15, IFIT1, IFI27, STAT*1; Fig. 1C; supplementary material Table S1. To confirm the array results, we measured by qRT-PCR the mRNA amounts of 15 upregulated genes related to inflammation (*S100A9, Il1F6, IFI27, OAS1A, CCL1, CCL20, LCN2, CASP1*), differentiation (*FLG, SPRR2A*), and other functions (*CAR2, SERPINB3A, STF3A, ATP12A*) in the epidermis of control and *RAC1*-mutant mice (Fig. 1D). All genes were stronger expressed in *RAC1*-null keratinocytes, although the variation was relatively high in the *RAC1*-null samples. These data confirm that loss of *RAC1* in keratinocytes *in vivo* increases expression of immune response and keratinocyte differentiation genes.

Loss of *RAC1* leads to changes in gene expression in both basal and supra-basal keratinocytes

Mouse epidermis contains basal keratinocytes, suprabasal keratinocytes, and immune cells. Since loss of *RAC1* leads to a slight increase in suprabasal cells (Chrostek et al., 2006), the increased expression of differentiation markers could be an effect of an increased number of suprabasal cells rather than a change in gene expression of individual cells. Moreover, altered numbers or activation of immune cells might contribute to the observed changes in gene expression in epidermis of mice lacking *RAC1* in keratinocytes.

We therefore sorted epidermal cells from adult control and *RAC1* mutant mice into basal keratinocytes (α6 integrin high, CD45−), suprabasal keratinocytes (α6 integrin low, CD45−), and immune cells (CD45+) and analyzed in the keratinocyte fractions the expression of 12 genes, which are upregulated in *RAC1*-null epidermis.

FACS analysis confirmed an increase in suprabasal cell numbers in *RAC1*-null epidermis from 27.5% ±4.1% in control to 40.8% ±2.2% in *RAC1*-null (n=4/4). Of 12 genes tested, five showed an increase in both basal and suprabasal fractions (*SPRR2A, STF3A, S100A9, IFI27, OAS1A*; Fig. 2A), while seven genes were mainly increased in the suprabasal fraction (*FLG, LCN2, ATP12A, CAR2, SERPINB3A, CCL1, IL1F6*; Fig. 2A). These data indicate that both basal and suprabasal keratinocytes show signs of aberrant differentiation and increased expression of immune response related genes in the absence of *RAC1* and that the phenotype observed in *RAC1*-null epidermis cannot be explained by an increased percentage of normally differentiated suprabasal cells.

Increased activation but no increased numbers of immune cells in *RAC1*-null epidermis

Infiltration of immune cells is a hallmark of clinical inflammation. We therefore assessed, whether loss of *RAC1* in keratinocytes leads to an increased number of immune cells in the

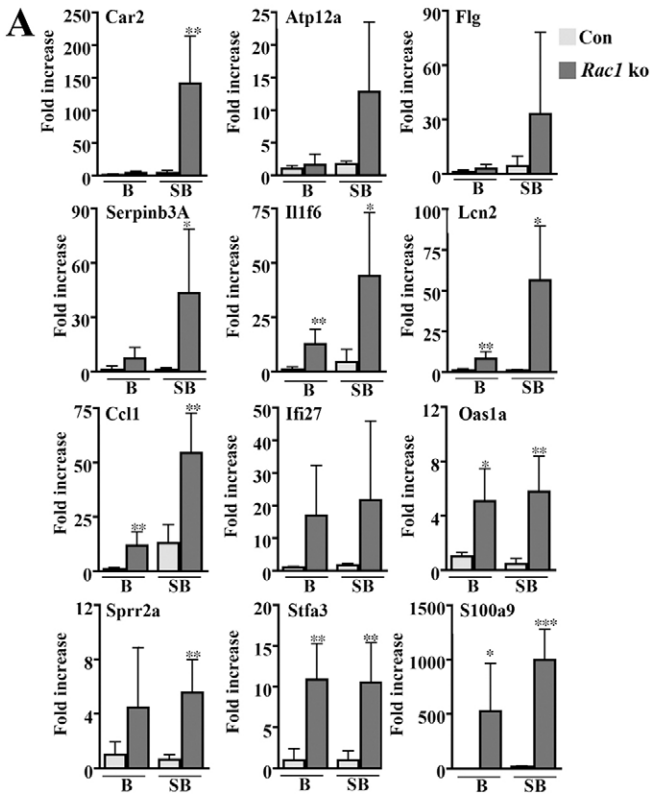

B

Gene	Rac1 ko fold
CD11b (Mac-1)	1
CD207 (langerin)	1.3
CD4	1.1
CD8	1
CD3	1.3
ICOS	5.8
Il17a	5.1
Ctla4	4.2
IFN-γ	3.9
CD69	3.8
CD18	3.2
CD11a	2.8
CD5	2.5
CCR6	2.5
CD28	2.5
CD11C	2.0

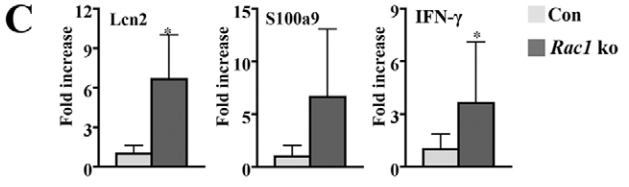

Fig. 2. Loss of *RAC1* in keratinocytes alters gene expression in basal and suprabasal keratinocytes and in epidermal immune cells. (**A**) Gene expression of 12 genes upregulated in *RAC1*-null epidermis by qRT-PCR in FACS-enriched basal (α6high CD45−) and suprabasal (α6low CD45−) keratinocytes of control and *RAC1*-null skin (n=4–5/4–5; **P*<0.05, ***P*<0.001, ****P*<0.0001). (**B**) Microarray gene expression analysis of selected immune cell markers in epidermis of *RAC1* ko mice compared with control mice identified by microarray (n=4/4). (**C**) Gene expression analysis by qRT-PCR of *LCN2*, *S100A9* and *INF-γ* in FACS enriched immune cells (CD45+) isolated from control and *RAC1*-null epidermis [n(LCN2, S100A9)=4/4; n(IFN-γ)=6/9; **P*<0.05].

epidermis of adult mice older than 2 months. It should be noted that the immune cells in our mice all express RAC1, since the deletion of the *RAC1* gene is restricted to the keratinocytes.

FACS analysis of CD45+ cells in the epidermis of adult mice did not indicate a significant increase in leukocytes in the absence of *RAC1* in keratinocytes (control: 4.1% ±1.9%; *RAC1* ko: 5.2% ±1.1%; n=14/14). Furthermore, checking the gene expression of markers for specific leukocyte subsets by microarray suggested unchanged numbers of T-cells (*CD4, CD8, CD3*), and macrophages (*MAC1*) in the epidermis (Fig. 2B). The marker for Langerhans cells (*CD207*) was not changed, but the dendritic cell marker *CD11C* appeared to be slightly increased (Fig. 2B). Expression of T-cell activation markers *ICOS, CTLA4, IL17A, CD69, CCR6, CD28* and *CD5* and of the T-cell expressed integrins *CD18 CD11A* was increased in *RAC1*-null epidermis (Fig. 2B). We noticed also a ~4-fold increase in *IFN-γ* expression, yet at a very low absolute level.

To validate this increase in *IFN-γ* message, we performed qRT-PCR analysis of different cell fractions of control and *RAC1* mutant epidermis. *IFN-γ* was about 3-fold elevated in immune cells isolated from *RAC1*-ko epidermis, confirming the result from the microarray analysis (Fig. 2C). No *IFN-γ* mRNA was detected in basal and suprabasal keratinocyte fractions of control and *RAC1* mutant mice. *IL-1β* and *IL6* mRNA were undetectable or low in keratinocytes and unchanged in keratinocytes and immune cells (supplementary material Fig. S2A,B).

We then assessed by qRT-PCR the contribution of immune cells to the increased expression of *LCN2*, *CCL1* and *S100A9* in *RAC1*-null epidermis. These genes have previously been described to be expressed by immune cells (Borregaard et al., 2007; Wiener et al., 2008; Yang et al., 2010). *LCN2* and *S100A9* displayed an increased expression in immune-cells isolated from *RAC1* ko epidermis, but the levels of expression were much lower than in keratinocytes (Fig. 2C). *CCL1* mRNA was strongly expressed, but not increased in immune cells in mutant mice compared to control mice (supplementary material Fig. S2C).

These data show that loss of *RAC1* in keratinocytes leads to activation of resident immune cells and a Th1 cytokine profile.

No observable changes in barrier function of *RAC1*-knockout mice

To reveal the mechanism of how loss of *RAC1* in keratinocytes leads to activation of immune cells we tested different hypotheses. First, we assessed whether it was possible to observe histological signs such as aberrant tight junctions that would support a defective barrier function of the epidermis, which could promote pathogen infiltration and immune cell activation. To optimally visualize the tight junctions at the transmission electron microscope, other than the routinely used OsO4, we utilized additional ruthenium and lanthanum based heavy metals in the post fixation process. We noticed in semithin sections that in the absence of the epidermal barrier, RuO4 diffused into the tissue resulting in black colorations (Fig. 3a,a′). This was primarily observed at the cut edges of the samples and to a very small extent in hair follicles. In the rest of the epidermis, black colorations did not diffuse deeper than the surface of the stratum corneum, suggesting a normal barrier function in *RAC1*-null skin (Fig. 3a,a′). Only in one isolated occasion, in one *RAC1* ko sample, deeper black colorations were observed. However, serial sections of the same sample as well as of two other *RAC1* ko and of one control sample revealed no diffusion from the surface and demonstrated the local restriction of this spot, which was probably due to sectioning of a peripheral region of the specimen.

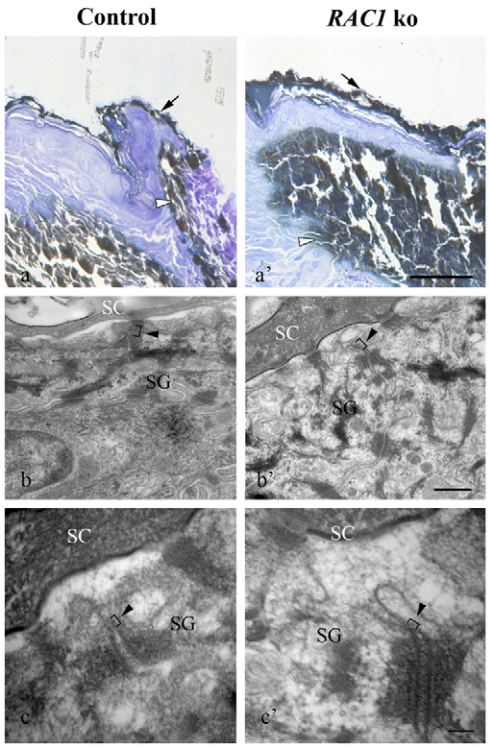

Fig. 3. No obvious ultrastructural signs of defective skin barrier of *RAC1* deficient mice. (**a**,**b**) Semithin sections of Control (a) and *RAC1* ko (b) mice after Os/Ru/La based post-fixation. Coloration was consistently seen in the surface of the stratum corneum (arrow) and also at the edges of the sample (white arrowhead). No differences in the level of penetration of the heavy metals from the surface or the edges of the tissue sample can be seen in the control and ko samples. (scale bar: 80 μm). (**c**−**f**) Ultrathin sections after Os/Ru/La based post-fixation. Tight junctions (black arrowhead pointing at the brackets) are clearly recognizable in the stratum granulosum (SG) in both control (c,e) and *RAC1* ko mice (d,f). Magnification in c is the same as shown in d (scale bar: 500 nm). Magnification in e is the same as shown in f (scale bar: 100 nm). SC, stratum corneum.

For the ultrastructural analysis, as it is effectively the first tight junction barrier that exogenous factors would encounter in penetrating the epidermis, we concentrated our focus on the last layer of the stratum granulosum immediately deep to the stratum corneum. Here, for consistency, apical tight junctions located above desmosomes were studied and compared in both groups. Tight junctions with normal morphology and arrangement, with sharply defined kissing points of the membranes were constantly found in *RAC1*-null epidermis (Fig. 3b,c,b′,c′). Only sporadically (<5%), the kissing points of a tight junction were not visualized above the corresponding desmosome in *RAC1* ko tissue. We also examined the distribution of lamellar bodies and found that they can be consistently seen in both control and mutant epidermis to a comparable extent, although their amount may vary among the individual cells of the same epidermis (supplementary material Fig. S3a,a′). Also, their striation was similarly evident in both control and Rac1-null sections (supplementary material Fig. S3b,b′). Accordingly, vesicles of secretion of lipids in to the intercellular spaces (i.e. vesicles at the cell borders) and presence of secreted lipids between the upper epidermal cells were seen to a similar extent in control and ko (supplementary material Fig. S3c,c′). These data, which correlate with the normal lifespan and lack of spontaneous wounding and blistering of *RAC1* ko mice, do not support a primary physical barrier defect as the driving factor behind the increased inflammatory response in mice with a keratinocyte specific ko of *RAC1*.

Loss of *RAC1* induces IFN response genes in keratinocytes in the absence of immune cells

We then tested the hypothesis, whether the aberrant differentiation and the increased expression of immune response genes observed in *RAC1*-null skin is secondary to the transient influx of inflammatory cells into the dermis of 14 d old *RAC1* ko mice, which leads to the removal of the lower part of the hair follicles (Chrostek et al., 2006).

We therefore studied gene-expression in full skin of 3 d old control and *RAC1* mutant mice. At this time point the deletion of the *RAC1* gene is complete, but no obvious hair follicle defect is visible in hematoxylin-eosin stained back skin sections and no sign of immune cell infiltration is observed (Chrostek et al., 2006). By microarray, we identified 697 genes upregulated more than 2-fold in skin from *RAC1* mutant mice. Remarkably, only two of these genes, the differentiation marker *SPRR1B* and the stress response gene *KRT16*, showed increased expression in the epidermis of adult *RAC1*-mutant mice. Grouping of the upregulated genes according to their function using the DAVID program did not identify any increase in groups related to keratinocyte differentiation or immune response. Instead, several groups of nuclear proteins were found to be elevated in skin of *RAC1*-mutant mice (supplementary material Fig. S4A).

The lack of any major signs of inflammation in 3 d old *RAC1* ko mice gave us the opportunity to culture keratinocytes independent from immune cells and any external inflammatory stimuli and study alterations in gene expression.

In contrast to *RAC1*-null keratinocytes from adult mice, *RAC1*-deficient keratinocytes from 3 d old mice spread and grew initially. After 4 d in culture, however, they showed signs of differentiation and stopped proliferation, corresponding to previous reports (Benitah et al., 2005). In order to investigate the changes in gene expression, we performed a microarray analysis of control and *RAC1* ko keratinocytes after 2 d culture *in vitro*.

557 genes were found to be upregulated more than 2-fold in *RAC1*-null keratinocytes and DAVID analysis indicated an increased expression of genes related to epidermal differentiation (Fig. 4A). 65 of the 231 genes upregulated in adult epidermis were also upregulated in 2 d cultured *RAC1* ko keratinocytes (supplementary material Table S2), including *S100A9* (3.5-fold), which is strongly upregulated in several human inflammatory diseases, *SPRR2A* (3.1-fold), which is a early skin differentiation marker, and the cysteine protease inhibitor *STFA3* (3.5-fold). Surprisingly, also interferon response genes such as *IFIT1* (4.3 fold), *ISG15* (4.6 fold), *CXCL10* (1.6 fold), and *STAT1* (3.2 fold) were increased in cultured *RAC1*-null keratinocytes. Importantly, STAT1 is not only an IFN response gene, but also a transcription factor activated by IFN signaling (Najjar et al., 2010). *CXCL10* is a known STAT1 target gene and an important activator of T-cells (Groom et al., 2011). *IFN-γ* expression, however, was indistinguishable from background levels and similar in control and *RAC1*-null keratinocytes. qRT-PCR confirmed a significantly increased expression of *S100A9*, *SPRR2A*, *STFA3*, *CXCL10*, and *STAT1* (Fig. 4B). Western blot analysis demonstrated that STAT1 is also increased at protein

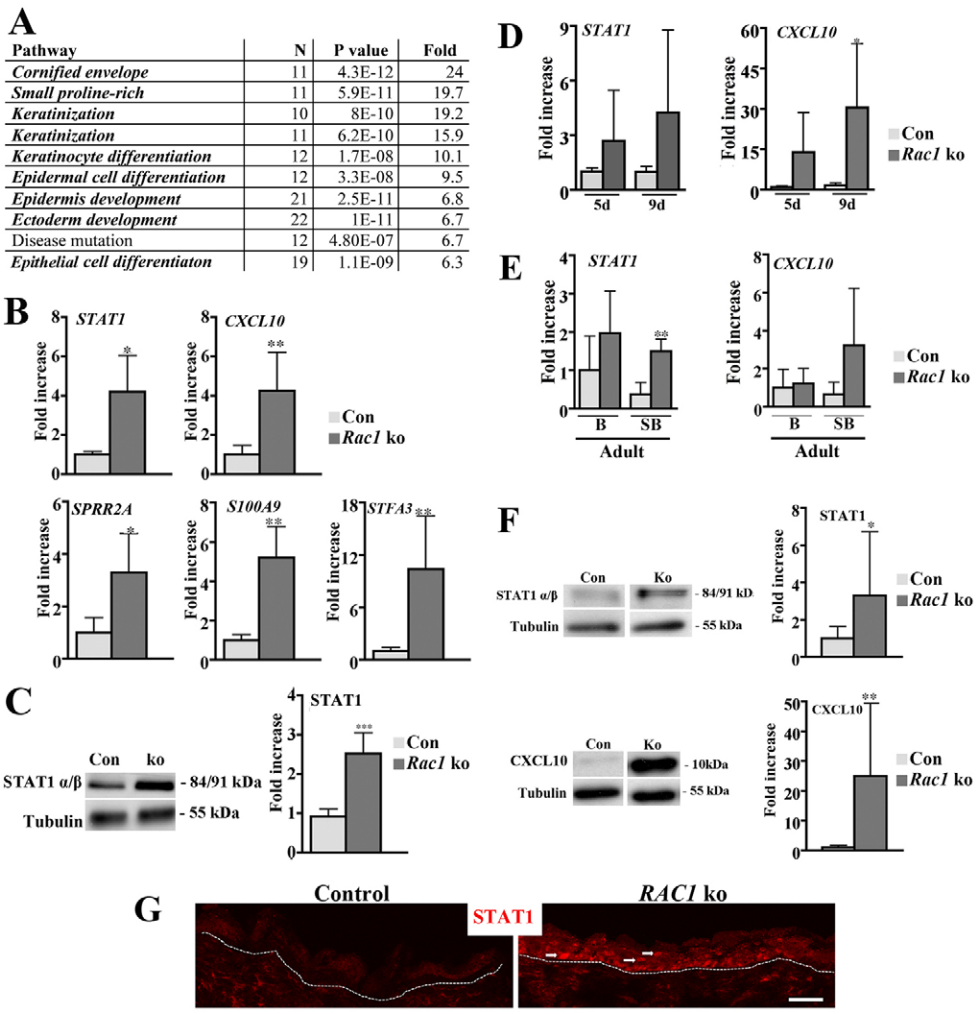

Fig. 4. Increased interferon response *in vivo* and *in vitro* in *RAC1* null cells. (**A**) Functional grouping of 557 genes increased more than twofold in *RAC1*-null keratinocytes isolated from 3 d old mice cultured for 2 d compared to control cells using the DAVID program. Bold italics indicates gene groups related to keratinocyte differentiation. 'N' indicates the number of genes in the group. 'Fold' indicates the fold enrichment of the group compared with a similar number of random genes [n=3(pooled)/3(pooled)]. (**B**) Gene expression analysis by qRT-PCR of *S100A9*, *STFA3*, *SPRR2A*, *STAT1*, and *CXCL10* in keratinocytes isolated from 3 d old control and Rac1 mutant mice cultured for 2 d *in vitro* [n(STAT1)=3/3; n(S100A9, STFA3, SPRR2A)=5/5; n(CXCL10)=6/6]. (**C**) Expression of STAT1 protein in keratinocytes isolated from 3 d old control and *RAC1* mutant mice cultured for 2 d *in vitro*. A representative western blot is shown (n=6/6; *P<0.05, **P<0.001, ***P<0.0001). (**D**) Gene expression analysis of *STAT1* and *CXCL10* in full skin samples from 5 day and 9 day old *RAC1* ko and control mice (n=6/6; *P<0.05). (**E**) Gene expression analysis for *STAT1* and *CXCL10* in FACS-enriched basal (α6high CD45−) and suprabasal (α6low CD45−) keratinocytes of control and *RAC1*-null skin (n=4–5/4–5; *P<0.05, **P<0.001). (**F**) Western blot analysis for STAT1 and CXCL10 in epidermal lysates from adult *RAC1* mutant mice and control mice. Representative western blots are shown (n=9/12; *P<0.05, **P<0.001. (**G**) Immunostaining for STAT1 on cryo-sections of back skin from adult control and *RAC1* mutant mice. The dashed line marks the dermal-epidermal junction. Representative pictures are shown (n=7/7).

level (Fig. 4C). These data suggest that the increased expression of IFN-γ response genes in cultured *RAC1*-null keratinocytes is independent of IFN-γ, but maybe related to the increased expression of the IFN-γ signal transducer STAT1.

Therefore, we checked more carefully the expression of *STAT1* and its target gene *CXCL10* in *RAC1*-null epidermis *in vivo*. qRT-PCR revealed increased expression of both *STAT1* and *CXCL10* in *RAC1*-null skin already in 5 d and 9 d old mice, thus preceding the transient influx of macrophages at 2 w of age (Fig. 4D). Expression levels in mutant samples were always higher than in control, but had a high variation. In adult epidermis, *STAT1* and *CXCL10* mRNA were particularly elevated in suprabasal keratinocytes lacking *RAC1* (Fig. 4E). Western blot analysis indicated significantly increased protein levels of STAT1 and CXCL10 in adult *RAC1*-null epidermis (Fig. 4F). Finally, immunofluorescent staining of back skin sections confirmed increased amounts of nuclear STAT1 in the absence of RAC1 *in vivo* (Fig. 4G).

These data show that increased expression of STAT1 is an early event *in vivo* that might contribute to the increased production of IFN-γ target genes such as CXCL10.

The increase in STAT1 is a cell autonomous effect independent of classical interferon signaling

To exclude that the increase in IFN response genes observed in cultured *RAC1*-null keratinocytes is a delayed onset phenotype dependent on interaction with immune cells *in vivo*, we isolated

not recombined, *RAC1* conditional keratinocytes from adult *RAC1 fl/fl* mice and induced the deletion of the *RAC1* gene by transfection with a cre and GFP expressing plasmid. Two days after transfection, GFP+ cells were sorted and replated. After two days in culture, we could detect a strong reduction of RAC1 protein (Fig. 5A) and a significant increase of STAT1 mRNA and protein as assessed by qRT-PCR and western blotting (Fig. 5B). This experiment confirms that the increase of STAT1 in *RAC1*-null keratinocytes is cell autonomous.

This increased expression of STAT1 in *RAC1*-null keratinocytes was unexpected, as RAC1 has not previously been described to regulate STAT1 levels. A known pathway to induce STAT1 expression is IFN-γ signaling. Binding of IFN-γ to the IFN-γ receptor leads to phosphorylation of the intracellular kinases JAK1 and JAK2, which activates STAT1. Activated STAT1-homodimers then translocate to the nucleus and induce expression of IFN-γ target genes including STAT1 (Najjar et al., 2010).

To investigate whether JAK1/2 activation is involved in the increased STAT1 expression observed in *RAC1*-null keratinocytes we performed western blotting for the phosphorylated forms of JAK1, JAK2 in lysates from 2 d cultured keratinocytes, isolated from 3 d old control and *RAC1* mutant mice. The levels of pJAK1 and pJAK2 were similar in control and *RAC1* ko keratinocytes (Fig. 5C). These experiments suggest that the increase of STAT1 in *RAC1* ko keratinocytes is not caused by an increase of classical interferon signaling.

RAC1-knockout keratinocytes show an increased interferon response after IFN-γ stimulation

The increase of STAT1 in keratinocytes might not only promote the expression of IFN response genes in keratinocytes, but could also increase the sensitivity of keratinocytes towards IFN-γ. To test this possibility, we stimulated control and *RAC1* ko keratinocytes for 6 h with two different concentrations of IFN-γ and thereafter tested by qRT-PCR the expression of the interferon response genes *CXCL10* and *IFIT1*. At all concentrations tested, *RAC1* ko keratinocytes showed a stronger response than control cells (Fig. 5D). This was observed both with keratinocytes isolated from 3 d old *RAC1*-null mice and with *in vitro* generated *RAC1*-null keratinocytes. IFN-γ treatment, however, did not affect expression of *SPRR2A*, *STFA3* or *S100A9* (supplementary material Fig. S4B), suggesting that expression of these aberrant keratinocyte differentiation markers is independent of STAT1. The increased expression of IFN-γ response genes correlated with an increased phosphorylation of STAT1 at tyrosine 701 (Fig. 5E), although STAT1 can activate gene expression also independent of this phosphorylation site (Cheon et al., 2009), e.g. by acetylation (Krämer et al., 2009), sumoylation (Begitt et al., 2011) other phosphorylations (Nguyen et al., 2001). These data indicate that the increase of STAT1 in *RAC1*-null keratinocytes is functionally relevant for the keratinocyte response to IFN-γ.

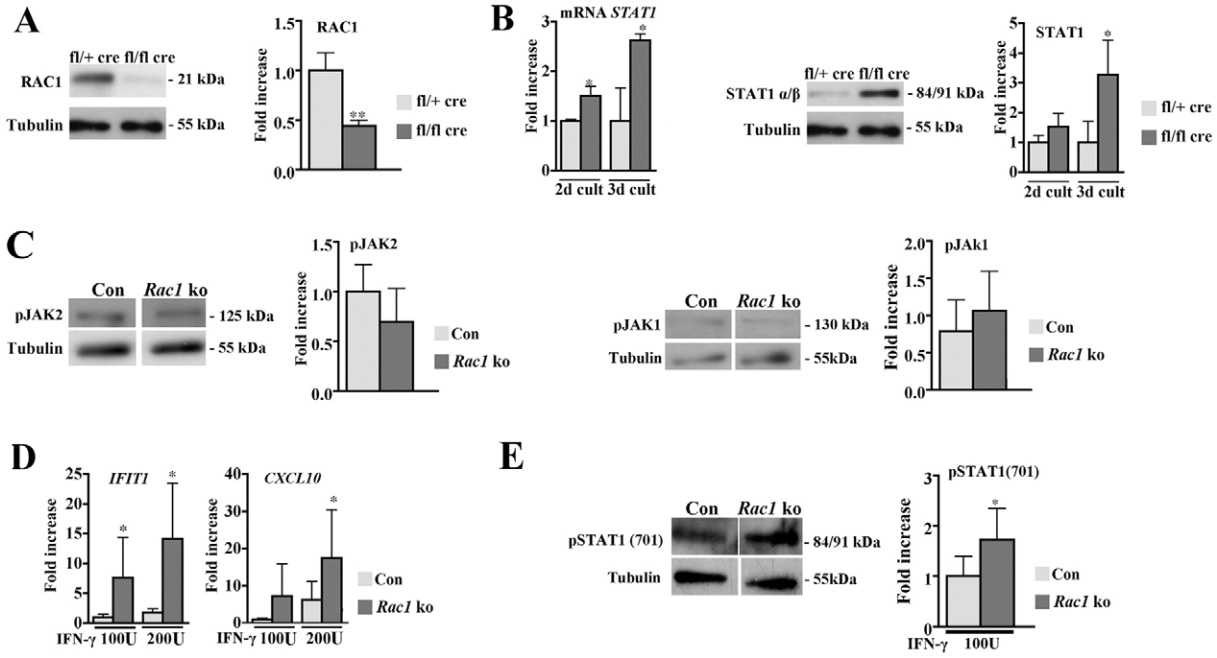

Fig. 5. Loss of *RAC1* in keratinocytes cell autonomously increases STAT1 expression and enhances sensitivity to IFN-γ. (**A**) Efficient loss of RAC1 protein in GFP+, cre transfected *RAC1 fl/fl* and *RAC1 fl/+* keratinocytes 4 d after transfection. Shown is a representative western blot and quantification of three independent experiments. (**B**) Gene expression analysis of GFP+, cre transfected *RAC1 fl/fl* and *RAC1 fl/+* keratinocytes 4 d after transfection for mRNA by qRT-PCR (left) and protein by western blot (right) for STAT1 and CXCL10. Representative western blots for 3 d are shown (middle; $n=3$–5/3–5). (**C**) Western blot analysis of pJAK2 (Tyr1007/1008) and pJAK1 (Tyr1022/1023) expression in keratinocytes isolated from 3 d old control and *RAC1* mutant mice cultured for 2 d *in vitro*. Shown is a representative western blot and quantification of three independent experiments. (**D**) Gene expression analysis by qRT-PCR of *CXCL10* and *IFIT1* mRNA in keratinocytes isolated from 3 d old control and *RAC1* mutant mice cultured for 2 d *in vitro* and stimulated for 6 h with indicated amounts of INF-γ ($n=5/6$; $^*P<0.05$, $^{**}P<0.001$). (**E**) Western blot analysis of pSTAT1 (Tyr 701) on subconfluent keratinocytes isolated from 3 d old control and *RAC1* ko mice cultured for 3 d *in vitro* and stimulated with 100 U/ml IFN-γ for 6 h ($n=6/8$; $^*P<0.05$).

Decreased F-actin polymerization in keratinocytes induces STAT1 expression, aberrant differentiation, and increased sensitivity to IFN-γ

To understand the molecular pathways mediating the RAC1 dependent control of STAT1 expression and aberrant differentiation, we next investigated, which signaling pathways are altered in *RAC1*-null keratinocytes cultured *in vitro*. *In vivo*, we reported earlier that RAC1 is crucial for hyperproliferation and the hyperactivation of PAK1/2, AKT and ERK in response to TPA treatment of the skin, though dispensable for normal activation of these molecules in untreated skin (Wang et al., 2010). Since the *in vitro* culture conditions correspond to hyperproliferative conditions *in vivo*, we tested these pathways in *RAC1*-null keratinocytes *in vitro*. Indeed, we found decreased activation of PAK1/2, AKT and ERK, as revealed by western blotting for phosphorylated forms of these molecules (Fig. 6A). Interestingly, total amounts of ERK and PAK1 were increased, whereas PAK2 and Akt were not changed (supplementary material Fig. S5). Since RAC1 is known to control Arp2/3 dependent actin polymerization via the WAVE complex (Steffen et al., 2004), we then assessed the organization of the actin cytoskeleton in 2 d cultured *RAC1*-null keratinocytes. *RAC1* ko keratinocytes were smaller and more elongated, which correlated with an impaired ability of *RAC1* ko keratinocytes in forming lamellipodia (Fig. 6B). Correspondingly, the average amount of F-actin per cell as determined by FACS analysis of keratinocytes stained with fluorescently labeled phalloidin was decreased in the absence of *RAC1* (Con: 874±166; *RAC1* ko: 558±102; $n=5/2$; $P=0.06$) and the percentage of F-actin low cells was increased (Con: 14.2±6; *RAC1* ko: 28.5±0.7; $n=5/2$; $P=0.02$). These data indicate that loss of *RAC1* decreases actin polymerization in keratinocytes *in vitro*.

To investigate, how each of these pathways is influencing *STAT1* expression and aberrant differentiation in keratinocytes, we used different inhibitors to block activation of PAK (PAK18, IPA3), ERK (MEK inhibitor PD98059), AKT (PI3K inhibitor LY294002), and actin polymerization (Latrunculin A) in wildtype keratinocytes *in vitro*. After 24 h incubation, we tested expression of *SPRR2A*, *STFA3*, *S100A9*, *STAT1* and *CXCL10* by qRT-PCR to detect aberrant differentiation and

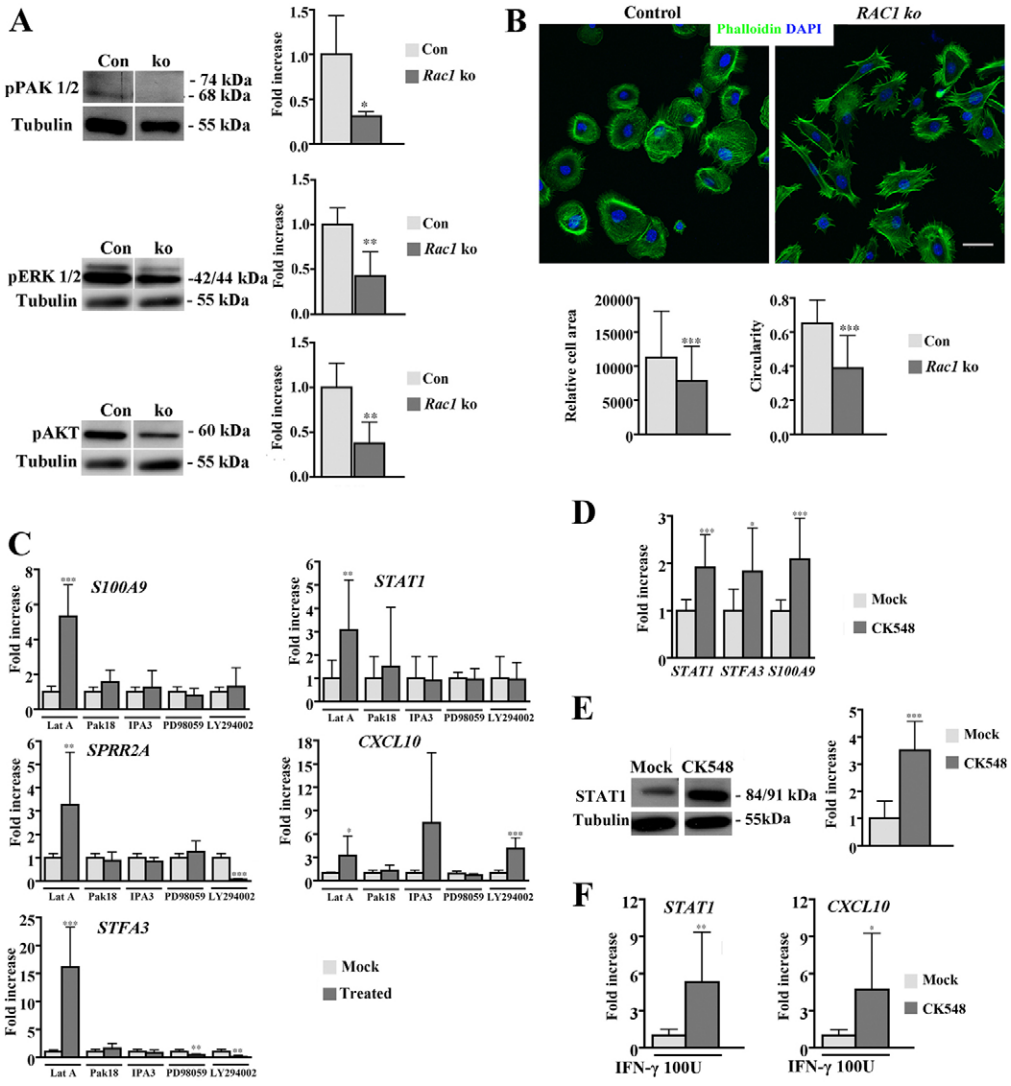

Fig. 6. Alterations in actin cytoskeleton correlate with increased STAT1 expression in keratinocytes *in vitro*. (**A**) Western blot analysis for pPAK1/2 (Thr423/Thr402), pERK1/2 (Thr202/Tyr204), and pAKT (Ser473) of lysates from keratinocytes isolated from 3 d old control and *RAC1* ko mice cultured for 2 d *in vitro* ($n=3–6/3–6$). (**B**) Phalloidin staining for F-actin by fluorescently labeled phalloidin in keratinocytes isolated from 3 d old control and *RAC1* ko mice cultured for 2 d *in vitro*. Nuclear counterstaining by DAPI. Shown are representative pictures ($n=1/6$; scale bar: 20 µm). Cell area and cell circularity (circle=1) were measured from 260 control and mutant keratinocytes. (**C**) Gene expression analysis of *STAT1*, *CXCL10*, *STFA3*, *S100A9* and *SRRR2A* by qRT-PCR in subconfluent control keratinocytes from adult mice treated for 24 h with either 0.5 µM latrunculin A, 10 µM Pak18, 10 µM IPA-3, 50 µM PD98059 or 50 µM LY294002 ($n=7–10/7–10$; $*P<0.05$, $**P<0.001$, $***P<0.0001$). (**D**) Gene expression analysis of *STAT1*, *STFA3*, and *S100A9* by qRT-PCR in subconfluent control adult keratinocytes treated for 24 h with 50 µM CK584 ($n=11/11$; $*P<0.05$, $**P<0.001$, $***P<0.0001$). (**E**) Western blot analysis for STAT1 in adult control keratinocytes after 24 h treatment with 50 µM CK548 ($n=6/6$; $***P<0.0001$) (**F**) Gene expression analysis of *STAT1* and *CXCL10* on 24 h 50 µM CK548 treated adult control keratinocytes after 6 h stimulation with 100 U/ml INF-γ ($n=8/9$; $*P<0.05$, $**P<0.001$).

increased expression of immune response genes. Inhibitors of PAK1/2, MEK and PI3K had either no or even an inhibitory effect on the expression of *SPRR2A*, *STFA3*, *S100A9* and *STAT1*. *CXCL10* expression was not affected by PAK18 or MEK inhibition, but increased by IPA3 and the PI3K inhibitor. However, disrupting actin dynamics by latrunculin increased the expression of all genes tested (Fig. 6C).

While latrunculin inhibits all actin polymerization, RAC1 is regulating particularly Arp2/3-mediated actin polymerization via the WAVE complex. To test whether Arp2/3 dependent actin polymerization is involved in regulation of gene expression, we applied the Arp2/3 inhibitor CK548 to wild-type keratinocytes *in vitro* and measured the mRNA expression of *STFA3* and *S100A9* and both mRNA and protein of STAT1 after 24 h. Arp2/3 inhibition significantly increased expression of all three genes (Fig. 6D,E). Interestingly, CK548 was less effective in upregulation of *STFA3* and *S100A9* than latrunculin or deletion of the *RAC1* gene (cf. Fig. 6D with Fig. 6C and Fig. 4C). As Arp2/3 inhibition increased STAT1 levels we tested if Arp2/3 treatment also makes cells more sensitive towards IFN-γ stimulation. Indeed, IFN-γ induced expression of *STAT1* and *CXCL10* was increased in CK548 treated control cells (Fig. 6F).

These data show that inhibition of Arp2/3 increases the expression of genes upregulated in *RAC1*-null cells and suggest that aberrant differentiation, increased expression of immune response related genes, and increased sensitivity towards interferons in *RAC1*-null keratinocytes are caused by changes in F-actin. In addition, inhibition of AKT or PAK1/2 might contribute to the increased expression of CXCL10 in *RAC1* ko keratinocytes.

RAC1 controls F-actin polymerization in keratinocytes *in vivo*

To assess whether *RAC1* is crucial for actin polymerization in keratinocytes also *in vivo*, we analyzed F-actin content in freshly isolated keratinocytes from 3 d and adult control and *RAC1* mutant mice. Average F-actin levels per cell were decreased both in 3 d old (Con: 215±34; *RAC1* ko: 157±32; $n=7/3$; $P=0.03$) and in adult mice (Con: 232±25; *RAC1* ko: 157±12; $n=3/3$; $P=0.01$). Similarly, the percentage of F-actin low cells was increased in *RAC1*-null keratinocytes at both time points (Fig. 7A), yet more pronounced in adult mice, where these changes were significant. Immunofluorescent staining for F-actin confirmed a decreased level of F-actin in epidermis of adult *RAC1* mutant mice compared to control (Fig. 7B).

This decreased actin polymerization *in vivo* corresponded to the increased expression of keratinocyte differentiation markers and immune response genes in adult *RAC1*-null epidermis.

Reduced actin polymerization stimulates expression of STAT1 and keratinocyte differentiation in a tanshinone dependent manner

To explore the mechanism how inhibition of actin polymerization affects gene expression in keratinocytes we tested different pathways.

Retinoic acid (RA) signaling was reported to upregulate STAT1 expression in a IFNγ independent manner (Wong et al., 2002; Shang et al., 1999; Kolla et al., 1997; Kolla et al., 1996). We therefore assessed whether inhibition of actin polymerization increases RA responsive element (RARE) dependent luciferase reporter expression and whether exogenous all-trans RA (ATRA) stimulates STAT1 expression in primary keratinocytes. While latrunculin treatment increased RARE activation more than twofold, the Arp2/3 inhibitor CK548 did not show an obvious effect (supplementary material Fig. S6A). ATRA treatment increased STAT1 expression in the presence of latrunculin, but neither alone, nor in the presence of CK548 (supplementary material Fig. S6B). These data do not support a major role of RA signaling in controlling STAT1 expression in response to RAC1-Arp2/3.

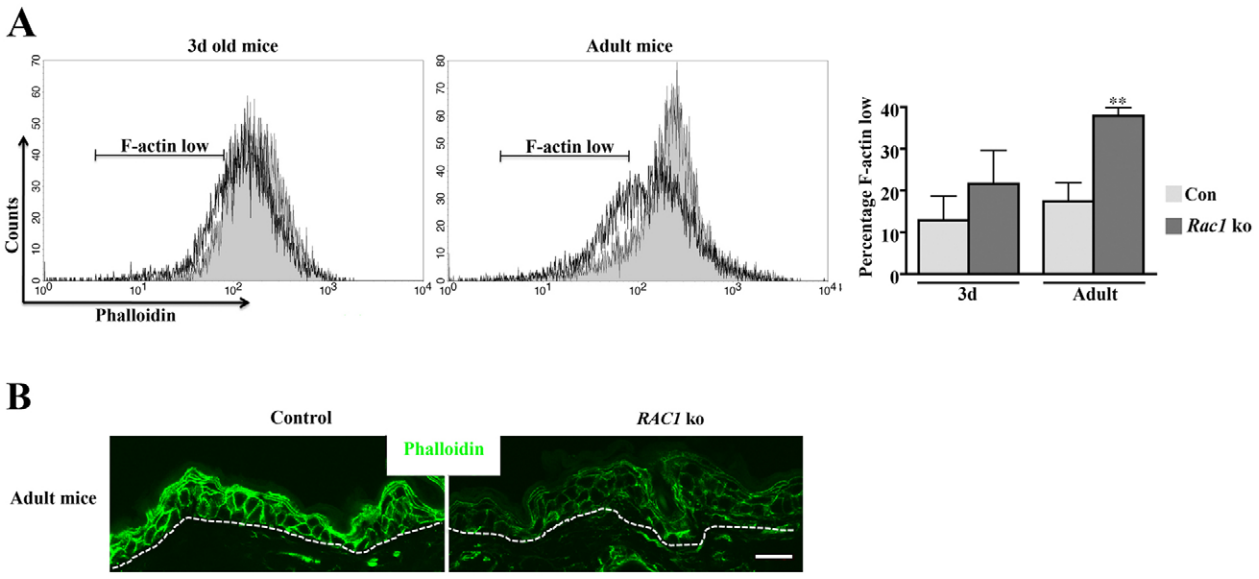

Fig. 7. Decreased actin polymerization in *RAC1*-null epidermis of adult mice. (**A**) Total F-actin levels in keratinocytes from 3 d old and adult control and *RAC1* ko mice determined by FACS analysis of primary keratinocytes stained with fluorescently labeled phalloidin and FITC-conjugated antibodies against α6 integrin [n(3 d)=6/3; n(adult)=3/3]; $^{**}P<0.001$). The percentage of F-actin low cells is shown in the bar chart. (**B**) F-actin levels in back skin of adult control and *RAC1*-mutant mice determined by staining with fluorescently labeled phalloidin. Representative pictures are shown ($n=3/3$; scale bar: 20 μm).

We then investigated the role of the AP-1 transcription factor, which promotes keratinocyte differentiation (Angel et al., 2001). AP-1 is a heterodimer of *JUN* and *FRA* family members and it was shown previously that inhibition of F-actin formation increases c-Jun expression by a posttranscriptional mechanism (Polak et al., 2006).

In 3 d old mice, no significant difference in c-Jun protein levels was observed (Fig. 8A). In adult *RAC1*-null epidermis, however, c-Jun protein amounts were threefold increased (Fig. 8A). Microarray gene expression analysis indicated no significant change in c-JUN mRNA in adult *RAC1*-null keratinocytes.

To inhibit AP-1 function we treated cultured keratinocytes with the AP-1 dimerization inhibitor tanshinone IIA. Tanshinone blocked latrunculin induced upregulation of *STAT1*, and largely prevented the increase in *S100A9* and *STFA3* (Fig. 8B). In the presence of tanshinone, the latrunculin induced increase of *S100A9* and *STFA3* was dramatically reduced (Fig. 8B). CK548 dependent regulation of *STAT1* on mRNA and protein level and *STFA3* expression was completely inhabitable by tanshinone,

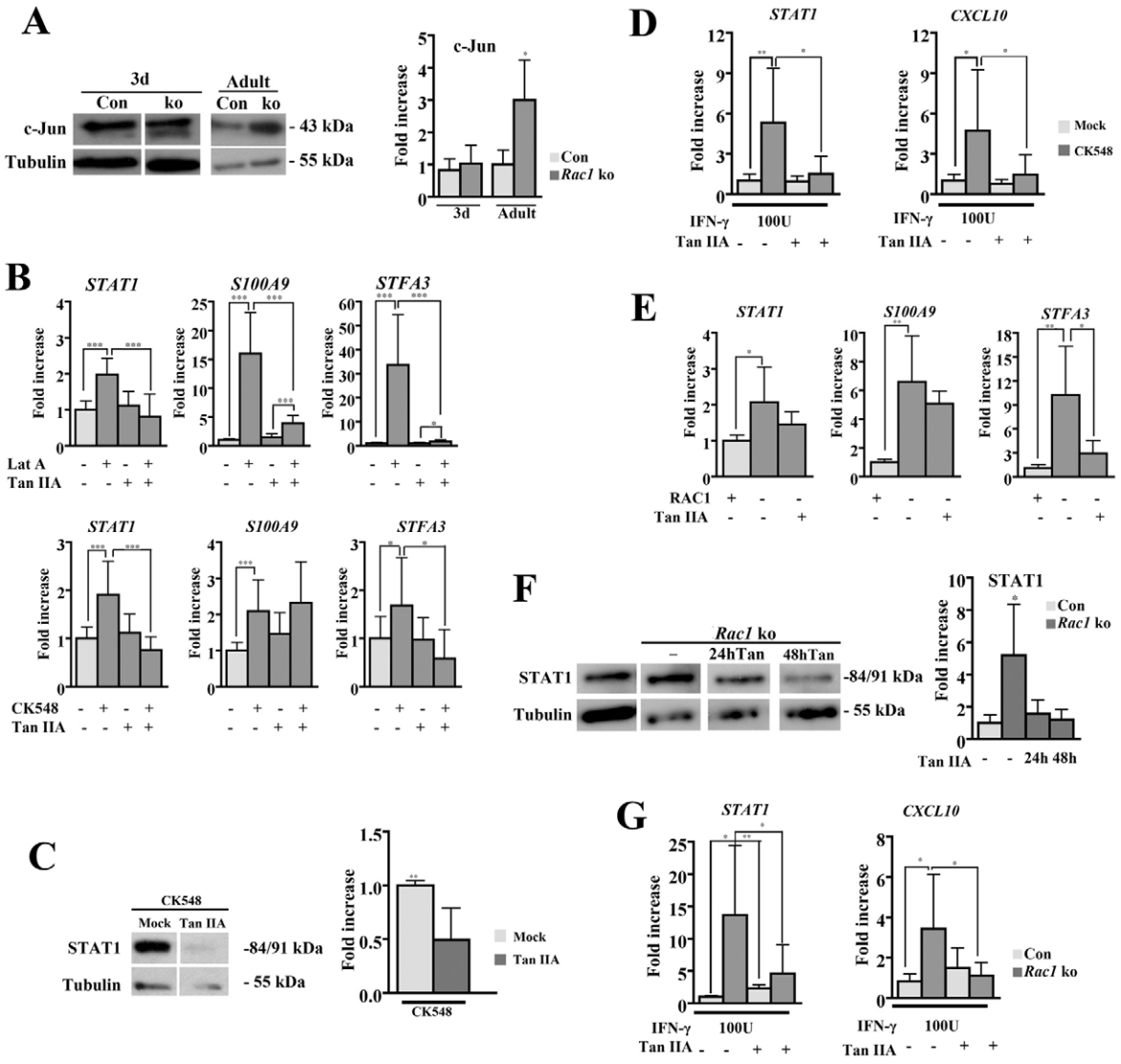

Fig. 8. RAC1 regulates actin polymerization-dependent gene expression in a tanshinone inhibitable manner. (**A**) Western blot analysis for c-JUN in epidermal lysates from 3 d old (n=4/4) and adult (n=5/5) *RAC1* ko mice. (**B**) Gene expression analysis of *STAT1*, *S100A9* and *STFA3* by qRT-PCR in subconfluent adult control cells treated with 3.5 µM tanshinone, 0.5 µM latrunculin or 50 µM CK584, as indicated (n=7/7; *P<0.05, **P<0.001, ***P<0.0001). (**C**) Western blot analysis of STAT1 expression in 24 h 50 µM CK548 and 3.5 µM tanshinone treated subconfluent adult control cells (n=6/6; **P<0.001). (**D**) Gene expression analysis of *STAT1* and *CXCL10* in 50 µM CK548 and 3.5 µM tanshinone treated subconfluent adult control cells stimulated for 6 h with 100 U/ml IFN-γ (n=9/8; *P<0.05, **P<0.001). (**E**) Gene expression analysis of *STAT1*, *S100A9* and *STFA3* in subconfluent keratinocytes from 3 d old control and *RAC1* ko mice cultured for 2 d *in vitro* and treated for 24 h with 3.5 µM tanshinone (n=3/3). (**F**) Western blot analysis for STAT1 expression in subconfluent keratinocytes isolated from 3 d old control and *RAC1* ko mice treated, cultured for 2 d *in vitro* and treated for indicated times with 3.5 µM tanshinone (n=3/3; *P<0.05; **P<0.001). (**G**) Gene expression analysis of *STAT1* and *CXCL10* in subconfluent keratinocytes from 3 d old control and *RAC1* mutant mice cultured for 3 d *in vitro* and treated for 48 h with 3.5 µM tanshinone and stimulated for 6 h with 100 U/ml IFN-γ (n=5/8; *P<0.05, **P<0.001).

while *S100A9* expression was not affected (Fig. 8B,C). Treatment with tanshinone alone did not alter gene expression (Fig. 8B,D).

Moreover, tanshinone also inhibited the increased interferon sensitivity observed after CK548 treatment (Fig. 8D). These data indicate that the increase in STAT1 expression is required for the CK548 induced increase of the IFN-γ response.

Despite the strong effect of the AP-1 inhibitor tanshinone, we could not observe a CK548 induced increase in c-Jun expression, suggesting a c-Jun independent mechanism at least *in vitro* (supplementary material Fig. S7).

Finally, we tested whether tanshinone is able to prevent the upregulation of *STAT1*, *S100A9* and *STFA3*, and the increased sensitivity towards interferons in primary *RAC1*-null keratinocytes cultured *in vitro*. Since freshly isolated neonatal keratinocytes show already certain changes, such as the reduced level of F-actin (Fig. 7A), it was not clear to what extent it would be possible to rescue the *RAC1*-null phenotype.

Similar to the CK548 treated cells, tanshinone strongly reduced the increase in *STFA3*, but showed no significant effect on *S100A9* (Fig. 8E). Average levels of *STAT1* mRNA were reduced and western blot analysis confirmed a reduction of STAT1 protein in tanshinone treated *RAC1*-null keratinocytes (Fig. 8F). Importantly, also the increased interferon response was inhibited by tanshinone treatment (Fig. 8G). These data strongly suggest that RAC1-Arp2/3 dependent regulation of actin polymerization controls expression of the keratinocyte differentiation markers, STAT1, and interferon sensitivity by a mechanism sensitive to tanshinone.

Discussion

Keratinocytes are able to produce a large number of different cytokines and chemokines such as IL1-β, IL1-α, IL6, IL10, IL18, TNF-α, Il1f6, CCL20, CXCl9, CXCL10 and CXCL11. These mediators promote the activation and infiltration of immune cells, which in turn secrete cytokines that affect keratinocyte gene expression and function. This positive feedback allows quick and efficient activation of the immune system in case of wounding or infection of the epidermis (Nestle et al., 2009).

Clearly, immune cells can trigger this crosstalk, as shown by the induction of psoriasiform, inflammatory skin lesions in mice by transfer of CD4+CD45RBhi T cells into T cell deficient *Rag2*−/− mice (Leon et al., 2006). However, also keratinocytes are able to initiate immune system activation. For example, overexpression of a constitutively active form of STAT3 in keratinocytes is sufficient to induce a psoriasis-like skin phenotype including infiltration of lymphocytes and neutrophils (Sano et al., 2005). Immune cell produced cytokines such as IL-6 or IFNs, on the other hand, are strong activators of STAT3 (Sano et al., 2005). Furthermore, keratinocyte-restricted deletion of the transcription factor AP-1 genes *JUNB* and *C-JUN* is causing a psoriasis-like inflammatory skin disease in mice by decreased expression of TIMP-3, which results in increased shedding of TNFα (Guinea-Viniegra et al., 2009). Finally postnatal loss of the transcription factor SRF resulted in a hyperproliferative skin disease with psoriasis-like lesions (Koegel et al., 2009).

We now describe an additional pathway, how keratinocytes can activate the immune system and contribute to skin inflammation. Loss of *RAC1* in keratinocytes induced cell autonomously the expression of the IFN-γ signal transducer STAT1, which conceivably increased the expression of immune cell activating proteins and chemokines such as CXCL10. In addition, the increased levels of STAT1 made *RAC1*-null keratinocytes hypersensitive to IFN-γ produced by immune cells, promoting the positive feedback loop by which keratinocytes increase immune cell activation. Many signaling pathways such as growth factor receptors, integrins, and cytokine receptors regulate RAC1 activation. RAC1-GTP might therefore be a signal integrator, collecting information from different sources, which then determines the sensitivity of the keratinocytes toward IFN-γ.

Unexpectedly, we found that RAC1 regulates STAT1 expression and interferon sensitivity by Arp2/3 mediated actin polymerization, which RAC1 promotes by interacting with the WAVE complex (Ladwein and Rottner, 2008). The RAC1 downstream effectors PAK, ERK and AKT, which are all less activated in *RAC1*-null keratinocytes cultured *in vitro*, however, seem not to affect STAT1 expression. Since F-actin formation is controlled by many other molecules in addition to RAC1, it is conceivable that other pathways contribute to the regulation of skin sensitivity. However, the similar effect of latrunculin, which inhibits all actin polymerization, CK548, which blocks Arp2/3 dependent actin polymerization, and *RAC1* knockout on the expression of STAT1 and the sensibility towards interferons suggests a major, non-redundant function for RAC1-Arp2/3.

Actin polymerization controls STAT1 expression and interferon sensitivity in a tanshinone regulated manner, as the inhibitor efficiently blocked the effects of latrunculin, CK548, and Rac1 deletion on STAT1 expression and the increased interferon sensitivity. *In vivo*, loss of RAC1 caused a posttranscriptional upregulation of c-Jun, similar to a latrunculin induced posttranscriptional upregulation of c-Jun in cell lines (Polak et al., 2006). In cell culture, c-Jun expression was not upregulated in *RAC1* ko cells or in Arp2/3 treated cells. This suggests that either it is a different member of the AP-1 transcription factor family which is regulating the response *in vitro* or it is a matter of AP-1 activation rather than absolute levels. Finally, off-target effects of tanshinone have to be considered.

Arp2/3 dependent actin polymerization is also regulating the expression of STFA3 and S100A9. S100A9 is a multifunctional molecule with chemokine-like, pro-inflammatory functions (Gebhardt et al., 2006), which probably further increases the hypersensitive status of the *RAC1*-null skin. However, the Arp2/3 inhibitor CK548 is much less stimulating compared to latrunculin and loss of RAC1, which is in contrast to the control of *STAT1* expression where latrunculin CK548 and *RAC1* ko induced *STAT1* to a similar extent. This might indicate the involvement of Arp2/3 independent actin polymerization in the regulation of *S100A9* and *STFA3*. Furthermore, Arp2/3 and RAC1 dependent regulation of *S100A9* expression is not significantly blocked by tanshinone. These findings reveal that different molecular mechanisms are mediating the F-actin dependent regulation of gene expression in keratinocytes. They furthermore confirm that expression of aberrant keratinocyte differentiation markers in *RAC1*-null cells is not simply a consequence of increased STAT1 expression.

Which additional mechanisms might be involved? One additional mechanism could be RA signaling, which we found to be increased in keratinocytes treated with latrunculin. Classical NF-κB signaling, however, which is altered in different skin

inflammation models (Wullaert et al., 2011), was not changed in *RAC1*-null keratinocytes.

Already earlier RAC1 has been described to regulate gene expression in epithelial cells by controlling actin polymerization (Busche et al., 2008; Busche et al., 2010). In that case, RAC1 induced actin polymerization released the transcriptional co-factor MAL from G-actin, which translocates to the nucleus, binds to the transcription factor SRF, and induces MAL-SRF dependent gene expression. This MAL dependent gene expression is completely inhibitable by latrunculin, which leads to depolymerization of the actin cytoskeleton. In contrast, we found that latrunculin treatment or loss of *RAC1* induced STAT1 expression in keratinocytes. It is therefore very unlikely that SRF is involved in the increased STAT1 expression.

Our data suggest that signaling pathways regulating RAC1 or actin polymerization in keratinocytes can modulate the sensitivity towards inflammatory skin diseases. Based on our study, it will be interesting to test RAC1 activation levels in skin of patients suffering from inflammatory skin diseases.

In conclusion, we demonstrate for the first time a link between RAC1 activation, Arp2/3 dependent actin polymerization, STAT1 expression and IFN-γ signaling in keratinocytes, which might play an important role in the crosstalk between keratinocytes and immune cells in inflammation related skin diseases. Actin polymerization is also involved in RAC1 dependent, aberrant keratinocyte differentiation, indicating that changes in the actin cytoskeleton can influence multiple signaling pathways.

Materials and Methods

Mice

Mice with keratinocyte restricted deletion of the *RAC1* gene (*RAC1 fl/fl* K5 cre) on a 129Sv/C57BL6 outbred background were described previously (Chrostek et al., 2006). Adult mice were 2–6 months old. Litter mates were used as controls.

Keratinocyte isolation and culture

Keratinocytes were isolated according to Lichti et al. (Lichti et al., 2008) and either directly processed ('in vivo') or cultured ('in vitro') following standard procedures. Size and circularity of keratinocytes were determined with ImageJ (http://rsbweb.nih.gov/ij/).

For *in vitro* experiments, subconfluent, growing keratinocyte cultures were used. For inhibitor experiments keratinocytes were treated for 24 h or indicated times with 0.5 µM latrunculin A, 10 µM PAK18, 10 µM IPA-3, 50 µM PD98059, 50 µM LY294002, 50 µM CK584 (all Sigma), 3.5 µM tanshinone IIA (TOCRIS) or 0.001% DMSO (Sigma). For interferon stimulation, keratinocytes were treated for 6 h with 100 U or 200 U INF-γ (Peprotec). For ATRA stimulation, cells were treated for 24 h with 1 µM all-trans retinal (Sigma).

Inflammatory skin models

TPA induced skin inflammation was carried out as described earlier (Wang et al., 2010). For croton oil induced irritant dermatitis adult mice were anesthetized by isoflurane and 10 µl 2% croton oil (Sigma) in a 4:1 acetone/olive oil mixture was applied on both sides of the right ear. As a control, the left ear was treated only with 4:1 acetone/olive oil mixture. Mice were sacrificed after 8 h, and infiltration of granulocytes was assessed by immunofluorescent staining of cryosections as described below. All animal studies were carried out according to Danish rules of animal welfare.

Histological analysis

7 µm sections of ear and back skin were performed on a cryostat and stained as described previously (Lefever et al., 2010). The following antibodies were used: rat anti Ly-6G (Gr-1), FITC-conjugated rat anti CD49f (clone GoH3; all BD Biosciences), rabbit anti STAT1 rabbit anti c-Jun (Cell Signaling). As secondary agents Cy3-conjugated goat anti-rabbit and Cy5-conjugated streptavidin were used (all Jackson ImmunoResearch). F-actin was detected by Alexa-Fluor-488-coupled phalloidin (Invitrogen). Nuclear counterstaining was performed with DAPI (Sigma).

Images were analyzed with a DM RXA2 microscope, equipped with 20X HC PL Apo (NA 0.70), 40X HCX PL APO (NA 1.25-0.75) and 63X HCX PL APO (NA 1.40-0.60) objectives controlled by Leica Microsystems confocal software (version 2.61 Build 1537; all Leica Microsystems). Images of human samples were obtained by a Zeiss AxioImager M2 upright microscope using a Plan-Apochromat 20×/0.8 objective.

Deletion of the *RAC1* gene *in vitro*

Primary keratinocytes from *RAC1 fl/fl* and, as control, *RAC1 fl/+* mice were transfected at 30–40% confluence with pRRLSIN-Cre-IRES-EGFP (kindly received from Didier Trono, EPFL, Lausanne, Switzerland) using TransIT-Keratinocyte Transfection Reagent (Mirus) following the instructions of the manufacturer.

Ultrastructural analysis

After sacrifice, small pieces of back skin were taken from one control and two *RAC1* ko, 30-week-old-mice and fixed in 4% paraformaldehyde, 2% glutaraldehyde, in 0.1M Na-cacodylate buffer pH 7.4 supplemented with 2 mM $CaCl_2$. For post-fixation, in addition to the traditional 1% OsO_4 treatment, also protocols with different combinations of metals including, other than 1% OsO_4, also 0.25% RuO_4 with 0.25% $K_3Fe(CN)_6$, and, 2% $La(NO_3)_3$ were used. After dehydration in a graded ethanol series, samples were embedded in Agar low viscosity resin according to standard protocol (Jackson et al., 2011).

Semithin sections of 1 µm were cut with a Reichert–Jung ultramicrotome and stained with toludine blue. All semithin sections were examined using Leica-Leitz DMRXE Confocal Microscope and images were captured using a Leica DFC 300 FX camera with accompanying software. In total, seven samples from the control mouse and 14 samples from the *RAC1* ko mice were examined.

Ultrathin sections of 90–95 nm were cut with a Reichert-Jung ultramicrotome and collected on 200 mesh formvar-coated copper grids for extensive analysis of the superficial tight junctions. Sections were stained with uranyl acetate and lead citrate in a Leica EM AC20 stainer. Sections were then examined with a Hitachi H-7000 Electron Microscope fitted with a 1K Hamamatsu Digital Camera. Images were captured using AMTV542 Image Capture Engine software. In total, six samples from the control mouse and 10 samples from the *RAC1* ko mice were examined.

Microarray gene expression analysis and qRT-PCR

RNA from epidermal lysates was isolated using the GeneElute Mammalian Total RNA miniprep kit (Sigma). Full skin samples were stored in RNA later (Sigma) and homogenized by a Dounce homogenizer before applying to the GeneElute kit. A proteinase K step was included according to protocol of the manufacturer.

Micrarray gene expression analysis was carried out at the Copenhagen University Hospital Microarray Center using the GeneChip Mouse Genome 430 2.0 Array (Affymetrix). Functional grouping of the upregulated genes was carried out using the DAVID program (Huang et al., 2009).

For qRT-PCR analysis, RNA was reverse transcribed using the RevertAid H Minus First Strand cDNA Synthesis kit (Fermentas). qRT-PCR was performed on the Applied Biosystems 7300 Real Time PCR system using SYBR green incorporation following standard protocols. The Ct value was calculated based on duplicates and normalized to the housekeeping gene *CYCA*.

Biochemical analysis

Western blotting was performed according to standard protocols. The following antibodies were used: mouse anti RAC1 (clone 102; BD Biosciences), rabbit anti STAT1, rabbit anti pSTAT1 (Tyr 701), rabbit anti pPAK1/2 (Thr423/Thr402), rabbit anti pAKT (S473), rabbit anti pERK (Thr 202/Tyr 204), rabbit anti pNF-κB (S536), rabbit anti pJAK2 (Y1007/1008), rabbit anti pJAK1 (Y1022/1023), rabbit anti c-JUN (all Cell Signaling), goat anti CXCL10 (R&D Systems) and mouse anti tyrosinated tubulin (Y/L1/2; kindly provided by J. Wehland, Braunschweig, Germany). As secondary agents horseradish-peroxidase-coupled goat anti rabbit, goat anti mouse, and donkey anti goat antibodies were used (all Jackson ImmunoResearch). All results were quantified using TotalLab TL100 software (Nonlinear Dynamics). Tubulin was used to normalize for different protein amounts.

FACS analysis

Epidermal cell preparations were isolated as described above and stained following standard procedures using PE-conjugated rat anti CD45.2, and FITC-conjugated rat anti CD49f. Fc receptors were blocked by rat anti CD16/32 (all BD Biosciences). F-actin was detected by Alexa-Fluor-488-coupled Phalloidin (Invitrogen). The stained cells were sorted on a pre-cooled FACSaria Cell sorter (BD Biosciences).

Luciferase assay

Primary keratinocytes were transfected at 30–40% confluence with pGL3-RARE-luciferase construct (Addgene 13548; Hoffman et al., 2006) and pRL-TK-Renilla construct (Promega) using TransIT-Keratinocyte Transfection Reagent (Mirus) following the instructions of the manufacturer. Two days later cells were harvested

and Renilla and firefly luciferase activity was measured using the Dual-Luciferase Reporter Assay System (Promega) following the instructions of the manufacturer using a Lumat CB9597 (Berthold Technologies).

Statistics

Data are presented as means ± standard deviation, with error bars representing standard deviation. Statistical significance was determined by the two-tailed Student's *t*-test. Significant differences are indicated by asterisks.

Acknowledgements

We would like to thank Volkan Turan, Anna Fossum, and Gabriele Begemann for expert technical help, Dr Dider Trono and Dr T. Michael Underhill for plasmids, Dr Jürgen Wehland for antibodies, and Dr David Wallach for inspiring discussion. E.P. planned and performed experiments, analyzed data and wrote the manuscript. Z.W., A.S., L.R., T.W. and K.P. performed experiments and analyzed data. FQ and CB planned experiments, analyzed data and wrote the manuscript. There is no conflict of interest for any of the authors.

Funding

This work was supported by the Danish Research Council; the Novo Nordisk Foundation; the Danish Cancer Research Foundation; the Lundbeck Foundation; and the University of Copenhagen.

Supplementary material available online at
http://jcs.biologists.org/lookup/suppl/doi:10.1242/jcs.107011/-/DC1

References

Angel, P., Szabowski, A. and Schorpp-Kistner, M. (2001). Function and regulation of AP-1 subunits in skin physiology and pathology. *Oncogene* **20**, 2413-2423.

Begitt, A., Droescher, M., Knobeloch, K. P. and Vinkemeier, U. (2011). SUMO conjugation of STAT1 protects cells from hyperresponsiveness to IFNγ. *Blood* **118**, 1002-1007.

Benitah, S. A., Frye, M., Glogauer, M. and Watt, F. M. (2005). Stem cell depletion through epidermal deletion of Rac1. *Science* **309**, 933-935.

Borregaard, N., Sørensen, O. E. and Theilgaard-Mönch, K. (2007). Neutrophil granules: a library of innate immunity proteins. *Trends Immunol.* **28**, 340-345.

Busche, S., Descot, A., Julien, S., Genth, H. and Posern, G. (2008). Epithelial cell-cell contacts regulate SRF-mediated transcription via Rac-actin-MAL signalling. *J. Cell Sci.* **121**, 1025-1035.

Busche, S., Kremmer, E. and Posern, G. (2010). E-cadherin regulates MAL-SRF-mediated transcription in epithelial cells. *J. Cell Sci.* **123**, 2803-2809.

Bustelo, X. R., Sauzeau, V. and Berenjeno, I. M. (2007). GTP-binding proteins of the Rho/Rac family: regulation, effectors and functions in vivo. *Bioessays* **29**, 356-370.

Castilho, R. M., Squarize, C. H., Patel, V., Millar, S. E., Zheng, Y., Molinolo, A. and Gutkind, J. S. (2007). Requirement of Rac1 distinguishes follicular from interfollicular epithelial stem cells. *Oncogene* **26**, 5078-5085.

Castilho, R. M., Squarize, C. H., Leelahavanichkul, K., Zheng, Y., Bugge, T. and Gutkind, J. S. (2010). Rac1 is required for epithelial stem cell function during dermal and oral mucosal wound healing but not for tissue homeostasis in mice. *PLoS ONE* **5**, e10503.

Cheon, H. and Stark, G. R. (2009). Unphosphorylated STAT1 prolongs the expression of interferon-induced immune regulatory genes. *Proc. Natl. Acad. Sci. USA* **106**, 9373-9378.

Chrostek, A., Wu, X., Quondamatteo, F., Hu, R., Sanecka, A., Niemann, C., Langbein, L., Haase, I. and Brakebusch, C. (2006). Rac1 is crucial for hair follicle integrity but is not essential for maintenance of the epidermis. *Mol. Cell. Biol.* **26**, 6957-6970.

Gebhardt, C., Németh, J., Angel, P. and Hess, J. (2006). S100A8 and S100A9 in inflammation and cancer. *Biochem. Pharmacol.* **72**, 1622-1631.

Groom, J. R. and Luster, A. D. (2011). CXCR3 ligands: redundant, collaborative and antagonistic functions. *Immunol. Cell. Biol.* **89**, 207-215.

Guinea-Viniegra, J., Zenz, R., Scheuch, H., Hnisz, D., Holcmann, M., Bakiri, L., Schonthaler, H. B., Sibilia, M. and Wagner, E. F. (2009). TNFalpha shedding and epidermal inflammation are controlled by Jun proteins. *Genes Dev.* **23**, 2663-2674.

Hoffman, L. M., Garcha, K., Karamboulas, K., Cowan, M. F., Drysdale, L. M., Horton, W. A. and Underhill, T. M. (2006). BMP action in skeletogenesis involves attenuation of retinoid signaling. *J. Cell Biol.* **174**, 101-113.

Huang, W., Sherman, B. T. and Lempicki, R. A. (2009). Systematic and integrative analysis of large gene lists using DAVID bioinformatics resources. *Nat. Protoc.* **4**, 44-57.

Jackson, B., Peyrollier, K., Pedersen, E., Basse, A., Karlsson, R., Wang, Z., Lefever, T., Ochsenbein, A. M., Schmidt, G., Aktories, K. et al. (2011). RhoA is dispensable for skin development, but crucial for contraction and directed migration of keratinocytes. *Mol. Biol. Cell* **22**, 593-605.

Koegel, H., von Tobel, L., Schäfer, M., Alberti, S., Kremmer, E., Mauch, C., Hohl, D., Wang, X. J., Beer, H. D., Bloch, W. et al. (2009). Loss of serum response factor in keratinocytes results in hyperproliferative skin disease in mice. *J. Clin. Invest.* **119**, 899-910.

Kolla, V., Lindner, D. J., Xiao, W., Borden, E. C. and Kalvakolanu, D. V. (1996). Modulation of interferon (IFN)-inducible gene expression by retinoic acid. Up-regulation of STAT1 protein in IFN-unresponsive cells. *J. Biol. Chem.* **271**, 10508-10514.

Kolla, V., Weihua, X. and Kalvakolanu, D. V. (1997). Modulation of interferon action by retinoids. Induction of murine STAT1 gene expression by retinoic acid. *J. Biol. Chem.* **272**, 9742-9748.

Krämer, O. H., Knauer, S. K., Greiner, G., Jandt, E., Reichardt, S., Gührs, K. H., Stauber, R. H., Böhmer, F. D. and Heinzel, T. (2009). A phosphorylation-acetylation switch regulates STAT1 signaling. *Genes Dev.* **23**, 223-235.

Ladwein, M. and Rottner, K. (2008). On the Rho'd: the regulation of membrane protrusions by Rho-GTPases. *FEBS Lett.* **582**, 2066-2074.

Lefever, T., Pedersen, E., Basse, A., Paus, R., Quondamatteo, F., Stanley, A. C., Langbein, L., Wu, X., Wehland, J., Lommel, S. et al. (2010). N-WASP is a novel regulator of hair-follicle cycling that controls antiproliferative TGFβ pathways. *J. Cell Sci.* **123**, 128-140.

Leon, F., Contractor, N., Fuss, I., Marth, T., Lahey, E., Iwaki, S., la Sala, A., Hoffmann, V., Strober, W. and Kelsall, B. L. (2006). Antibodies to complement receptor 3 treat established inflammation in murine models of colitis and a novel model of psoriasiform dermatitis. *J. Immunol.* **177**, 6974-6982.

Lichti, U., Anders, J. and Yuspa, S. H. (2008). Isolation and short-term culture of primary keratinocytes, hair follicle populations and dermal cells from newborn mice and keratinocytes from adult mice for in vitro analysis and for grafting to immunodeficient mice. *Nat. Protoc.* **3**, 799-810.

Lowes, M. A., Bowcock, A. M. and Krueger, J. G. (2007). Pathogenesis and therapy of psoriasis. *Nature* **445**, 866-873.

Najjar, I. and Fagard, R. (2010). STAT1 and pathogens, not a friendly relationship. *Biochimie* **92**, 425-444.

Nestle, F. O., Di Meglio, P., Qin, J. Z. and Nickoloff, B. J. (2009). Skin immune sentinels in health and disease. *Nat. Rev. Immunol.* **9**, 679-691.

Nguyen, H., Ramana, C. V., Bayes, J. and Stark, G. R. (2001). Roles of phosphatidylinositol 3-kinase in interferon-gamma-dependent phosphorylation of STAT1 on serine 727 and activation of gene expression. *J. Biol. Chem.* **276**, 33361-33368.

Polak, P., Oren, A., Ben-Dror, I., Steinberg, D., Sapoznik, S., Arditi-Duvdevany, A. and Vardimon, L. (2006). The cytoskeletal network controls c-Jun translation in a UTR-dependent manner. *Oncogene* **25**, 665-676.

Sano, S., Chan, K. S., Carbajal, S., Clifford, J., Peavey, M., Kiguchi, K., Itami, S., Nickoloff, B. J. and DiGiovanni, J. (2005). Stat3 links activated keratinocytes and immunocytes required for development of psoriasis in a novel transgenic mouse model. *Nat. Med.* **11**, 43-49.

Shang, Y., Baumrucker, C. R. and Green, M. H. (1999). The induction and activation of STAT1 by all-trans-retinoic acid are mediated by RAR beta signaling pathways in breast cancer cells. *Oncogene* **18**, 6725-6732.

Steffen, A., Rottner, K., Ehinger, J., Innocenti, M., Scita, G., Wehland, J. and Stradal, T. E. (2004). Sra-1 and Nap1 link Rac to actin assembly driving lamellipodia formation. *EMBO J.* **23**, 749-759.

Tscharntke, M., Pofahl, R., Chrostek-Grashoff, A., Smyth, N., Niessen, C., Niemann, C., Hartwig, B., Herzog, V., Klein, H. W., Krieg, T. et al. (2007). Impaired epidermal wound healing in vivo upon inhibition or deletion of Rac1. *J. Cell Sci.* **120**, 1480-1490.

Wagner, E. F., Schonthaler, H. B., Guinea-Viniegra, J. and Tschachler, E. (2010). Psoriasis: what we have learned from mouse models. *Nat. Rev. Rheumatol.* **6**, 704-714.

Wang, Z., Pedersen, E., Basse, A., Lefever, T., Peyrollier, K., Kapoor, S., Mei, Q., Karlsson, R., Chrostek-Grashoff, A. and Brakebusch, C. (2010). Rac1 is crucial for Ras-dependent skin tumor formation by controlling Pak1-Mek-Erk hyperactivation and hyperproliferation in vivo. *Oncogene* **29**, 3362-3373.

Wiener, Z., Pocza, P., Racz, M., Nagy, G., Tolgyesi, G., Molnar, V., Jaeger, J., Buzas, E., Gorbe, E., Papp, Z. et al. (2008). IL-18 induces a marked gene expression profile change and increased Ccl1 (I-309) production in mouse mucosal mast cell homologs. *Int. Immunol.* **20**, 1565-1573.

Wong, L. H., Sim, H., Chatterjee-Kishore, M., Hatzinisiriou, I., Devenish, R. J., Stark, G. and Ralph, S. J. (2002). Isolation and characterization of a human STAT1 gene regulatory element. Inducibility by interferon (IFN) types I and II and role of IFN regulatory factor-1. *J. Biol. Chem.* **277**, 19408-19417.

Wullaert, A., Bonnet, M. C. and Pasparakis, M. (2011). NF-κB in the regulation of epithelial homeostasis and inflammation. *Cell Res.* **21**, 146-158.

Yang, J., Meyer, M., Müller, A. K., Böhm, F., Grose, R., Dauwalder, T., Verrey, F., Kopf, M., Partanen, J., Bloch, W. et al. (2010). Fibroblast growth factor receptors 1 and 2 in keratinocytes control the epidermal barrier and cutaneous homeostasis. *J. Cell Biol.* **188**, 935-952.

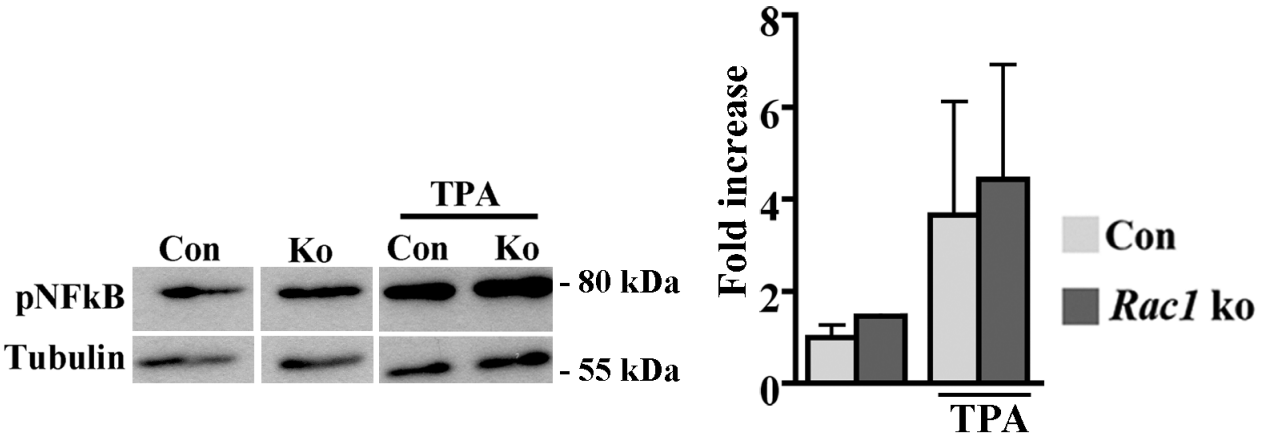

Fig. S1. Western blot analysis of epidermal lysates from untreated and two weeks TPA treated, adult control and *RAC1* ko mice for pNFκB (S536) (n (untreated)= 3/2; n (treated)= 3/3).

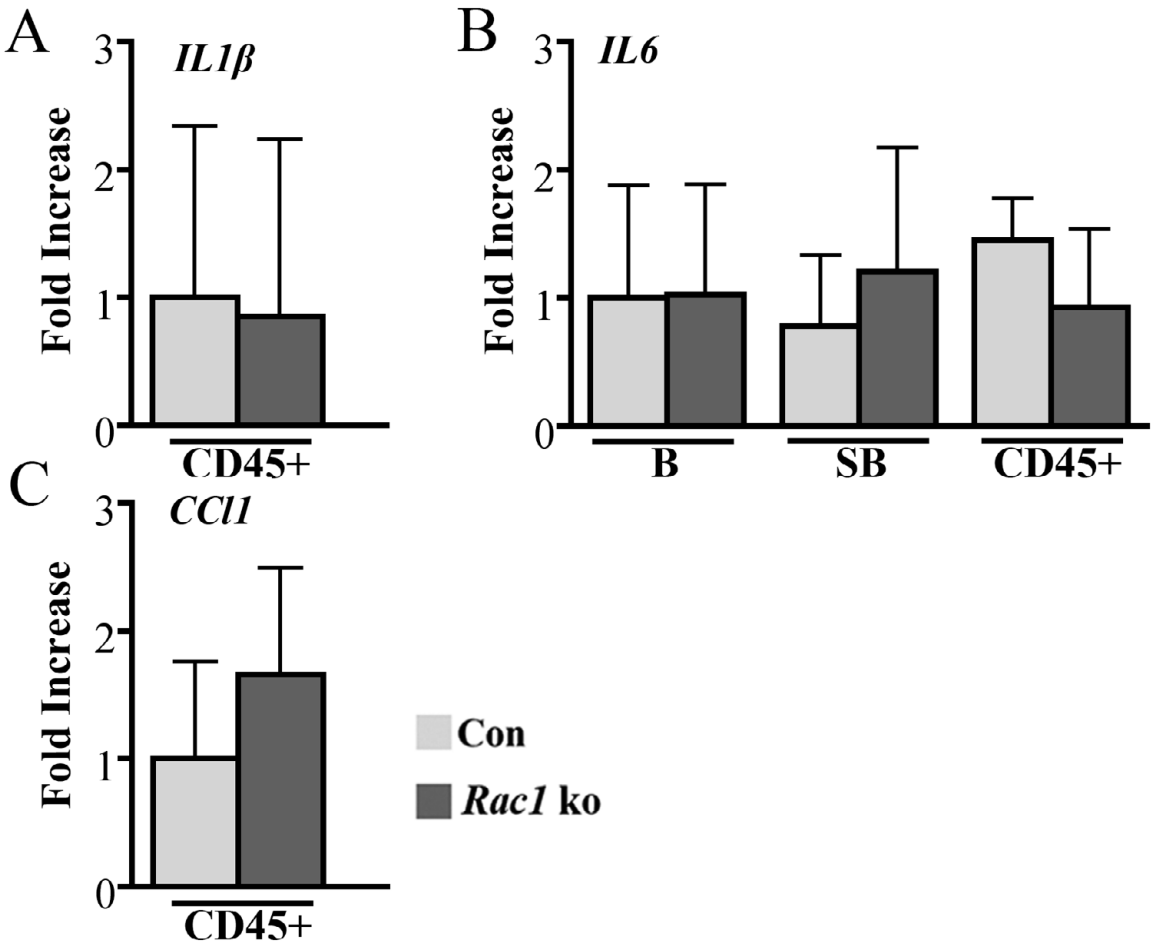

Fig. S2. (A) Gene expression of *IL1*β in FACS-enriched immune cells (CD45+) isolated from control and *RAC1*-null epidermis as determined by qRT-PCR (n=6/9); (B) *IL6* expression in FACS-enriched basal (α6high CD45-), suprabasal (α6low CD45-), and immune cells (CD45+), isolated from control and *RAC1*-null epidermis as determined by qRT-PCR (n= 3/3); (C) Gene expression of *CCL1* in FACS-enriched immune cells (CD45+) isolated from control and *RAC1*-null epidermis as determined by qRT-PCR (n=5/6).

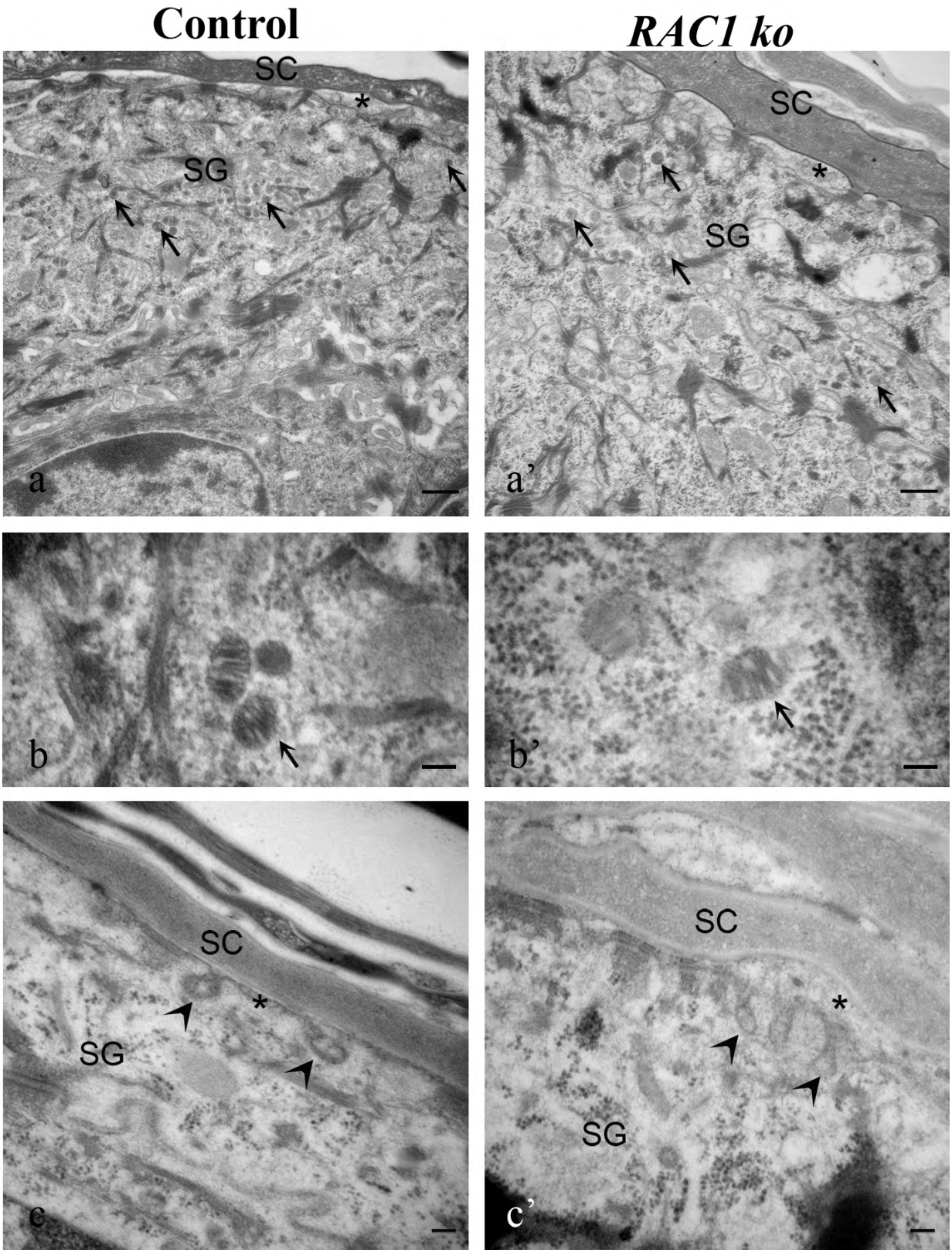

Fig. S3. Ultrathin sections of epidermis from 30 week old control (a, b, c) and *RAC1* ko mice (a', b', c') after La+Os+Ru (a+a´, b+b´) or Os+Ru (c+c´) based post fixation of the tissues show intracellular lamellar bodies (black arrows) and secretion of their contents (black arrowheads) to comparable extent. Asterisk= secreted material adjacent to the plates of the stratum corneum (SC). SG= stratum granulosum. Scale bars in a+a'= 500 nm, in b+b' and in c+c'= 100 nm.

A

Pathway	N	P value	Fold
Bromodomain conserved site	13	3.5E-11	14.2
Bromodomain	13	1.1E-10	13
Bromodomain	14	3E-11	12.5
BROMO	14	1.5E-09	9.1
Compositionally biased region:Lys-rich	24	8.5E-14	7.4
SANT, DNA-binding	10	8.80E-06	7.1
Zinc finger, CCCH-type	10	1.20E-05	6.8
High mobility group, HMG1/HMG2	10	1.20E-05	6.8
Nuclear speck	14	3.80E-07	6.1
Compositionally biased region:Arg-rich	16	1.20E-07	5.7

B

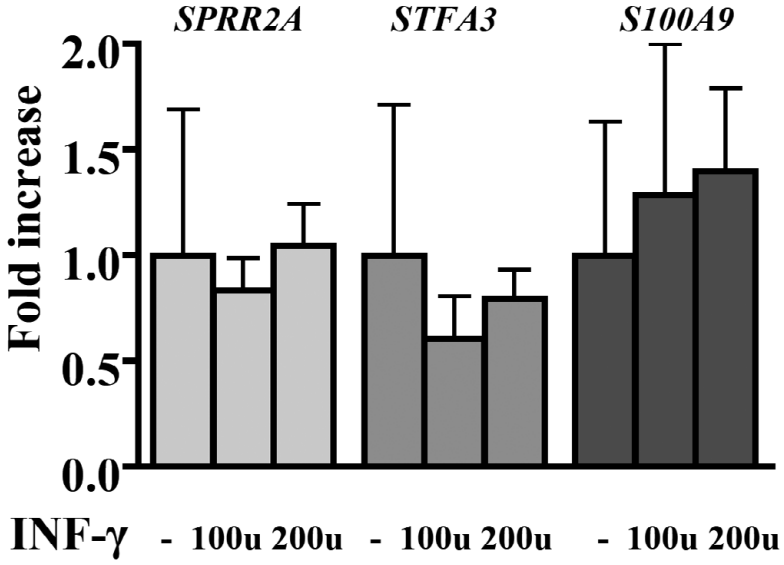

Fig. S4. (A) Functional grouping of 697 genes increased more than two-fold in the epidermis of 3d old *RAC1* ko mice compared to control mice using the DAVID program (Huang et al., 2009). "N" indicates the number of genes in the group. "Fold" indicates the fold enrichment of the group compared to a similar number of random genes (n=3 (pooled)/3(pooled)). (B) Gene expression of *SPRR2A*, *STFA3*, and *S100A9* in 2d cultured keratinocytes isolated from 3d old mice treated for 6h with 100U or 200U INF-γ (n=3).

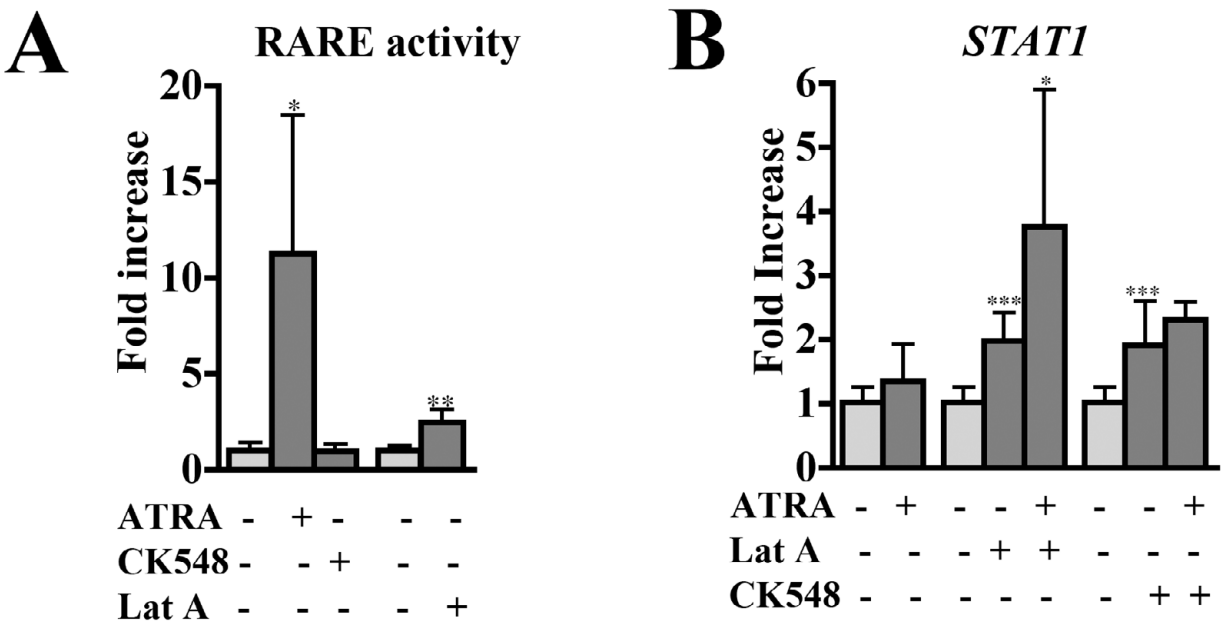

Fig. S5. Western blot analysis of subconfluent 2d cultured *RAC1* mutant and control keratinocytes isolated form 3d old mice for ERK, Akt, PAK1 and PAK2 (n= 6/6)

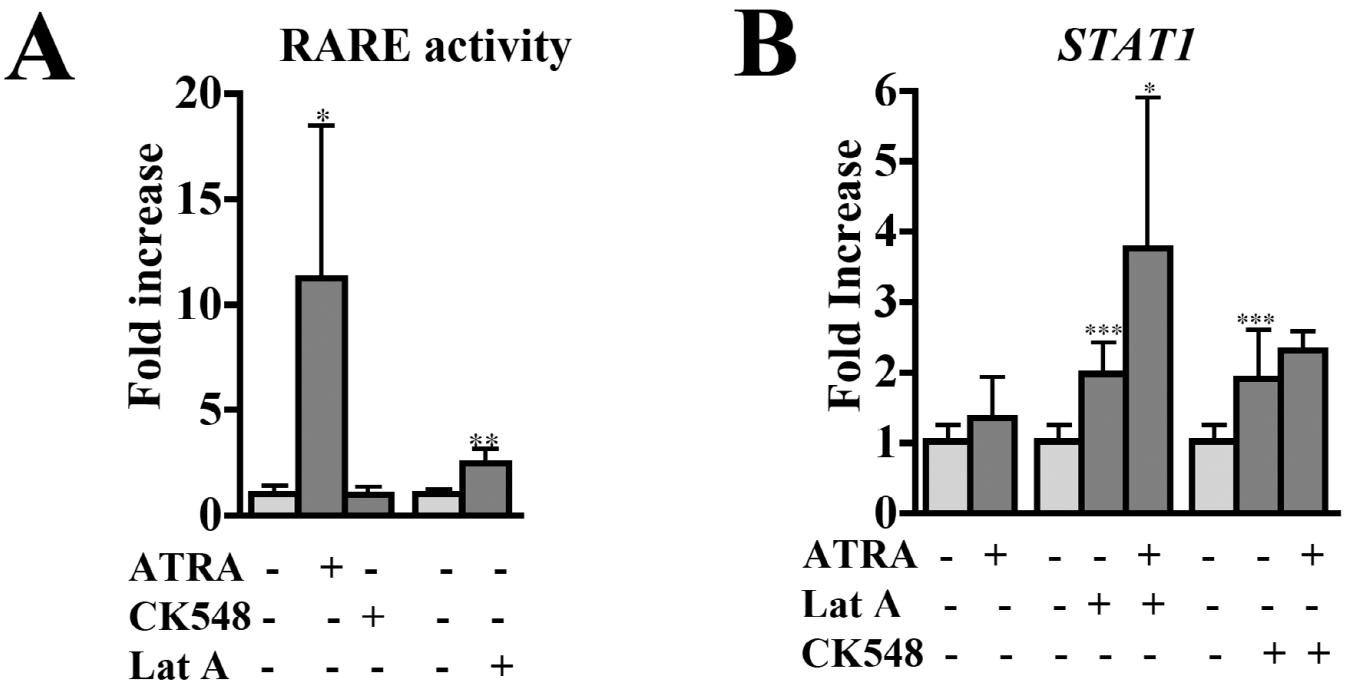

Fig. S6. RARE luciferase activity assay in control keratinocytes treated for 24h with 0.5μM latrunculin (n=9/9), 50μM CK584, and 1μM ATRA as indicated (n=6/6). (B) Gene expression analysis of *STAT1* by qRT-PCR in subconfluent control cells treated for 24h with 1μM ATRA, 0.5μM latrunculin, or 50μM CK584 (n=11/11).

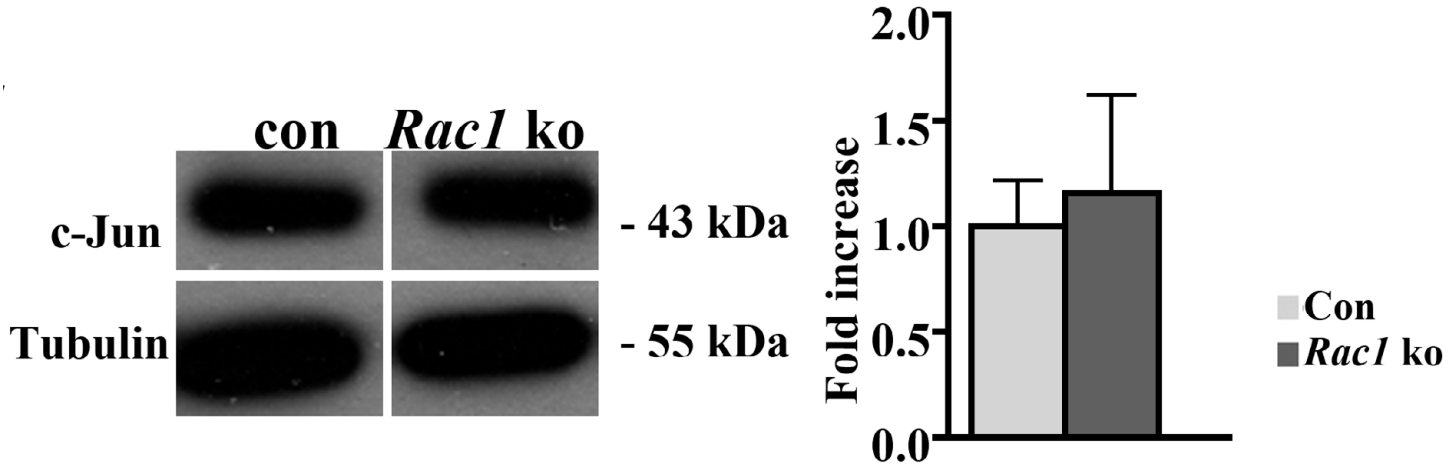

Fig. S7. Western blot analysis for c-Jun in subconfluent control kerationcytes from adult mice treated for 24hr with 50μM CK584 and 3.5 μM tanshinone IIA (n= 3/3)

Table S1.

Genes upregulated more than two-fold in *RAC1*-null epidermis compared to control, identified by microaray gene expression analysis (n=4/4)

Affymetrix ID	Gene symbol	Fold
1448756_at	S100a9	38.2
1419394_s_at	S100a8	32.0
1435639_at	2610528A11Rik	28.6
1426278_at	Ifi27l2a	23.1
1418580_at	Rtp4	16.0
1420771_at	Sprr2d	15.4
1419709_at	Stfa3	15.1
1422672_at	Sprr1b	13.2
1453196_a_at	Oasl2	13.2
1437258_at	Sprr2a	12.4
1420550_at	Lce1f	12.4
1422240_s_at	Sprr2h	11.0
1427268_at	Flg	10.7
1424518_at	Apol9a / Apol9b	10.6
1427747_a_at	Lcn2	10.0
1419591_at	Gsdmc	9.2
1451537_at	Chi3l1	9.1
1450791_at	Nppb	9.1
1450783_at	Ifit1	9.0
1421256_at	Gzmc	8.8
1451510_s_at	Olah	8.6
1419215_at	Aox4	8.5
1449475_at	Atp12a	8.5
1420676_at	Lce1a1	8.4
1456539_at	---	8.4
1434046_at	AA467197	7.8
1418609_at	Il1f6	7.0
1419498_at	Tmigd1	7.0
1449064_at	Tdh	6.9
1450618_a_at	Sprr2a	6.5
1437517_x_at	Serpinb3a	6.5
1424775_at	Oas1a	6.4
1435761_at	Stfa1	6.4
1435760_at	Csta	5.9

1429636_at	EG546347	5.8
1422588_at	Krt6b	5.7
1448932_at	Krt16	5.7
1424921_at	Bst2	5.6
1421688_a_at	Ccl1	5.5
1453218_at	Lce1c	5.5
1431591_s_at	Isg15	5.3
1449938_at	Pp11r	5.3
1418345_at	Tnfsf12-tnfsf13	5.3
1416847_s_at	Oas1d /Oas1e	5.2
1420562_at	Slurp1	5.1
1419409_at	Lce1b	5.1
1421672_at	Il17a	5.1
1422846_at	Rbp2	5.0
1420332_x_at	Lce1d	4.9
1450875_at	Gpr37	4.8
1420664_s_at	Procr	4.8
1438498_at	Zmynd15	4.7
1429862_at	Pla2g4e	4.7
1448380_at	Lgals3bp	4.7
1418648_at	Egln3	4.6
1419057_at	Slc5a1	4.6
1452492_a_at	Slc37a2	4.6
1425715_at	Il1f8	4.5
1415802_at	Slc16a1	4.5
1416854_at	Slc34a2	4.5
1454159_a_at	Igfbp2	4.5
1448752_at	Car2	4.5
1434372_at	AW112010	4.4
1429540_at	Cnfn	4.3
1448754_at	Rbp1	4.2
1448710_at	Cxcr4	4.2
1448745_s_at	Lor	4.2
1425374_at	Oas3	4.1
1416165_at	Rab31	4.1
1418173_at	Krt25	4.1
1420350_at	Lce1a2	4.1
1416514_a_at	Fscn1	4.0
1425958_at	Il1f9	4.0
1420741_x_at	Lce1i	4.0
1425606_at	Slc5a8	4.0
1428735_at	Cd69	4.0
1441054_at	Apol8	3.9

1419004_s_at	Bcl2a1a/ Bcl2a1b	3.9
1422029_at	Ccl20	3.9
1416306_at	Clca3	3.8
1451613_at	Hrnr	3.8
1452592_at	Mgst2	3.8
1424268_at	Smox	3.8
1422940_x_at	Serpinb3b / Serpinb3c	3.8
1448457_at	Krt71	3.8
1448982_at	Klk6	3.7
1456157_at	---	3.7
1451375_at	Ehf	3.6
1420722_at	Elovl3	3.6
1419684_at	Ccl8	3.6
1425065_at	Oas2	3.6
1417426_at	Srgn	3.6
1429960_at	4930438A08Rik	3.6
1424451_at	Acaa1b	3.5
1424549_at	Degs2	3.5
1449974_at	Gapdhs	3.5
1416287_at	Rgs4	3.5
1418937_at	Dio2	3.5
1428834_at	Dusp4	3.5
1449378_at	Krt27	3.4
1417697_at	Soat1	3.4
1434092_at	Atg9b	3.4
1460603_at	Samd9l	3.4
1450250_at	Otud7a	3.4
1451924_a_at	Edn1	3.3
1440990_at	Kif26b	3.3
1454264_at	2310046K23Rik	3.3
1443163_at	Slc39a2	3.3
1438868_at	D14Ertd668e	3.3
1418126_at	Ccl5	3.3
1418393_a_at	Itga7	3.3
1417292_at	Ifi47	3.2
1430641_at	Gsdmc2 / Gsdmc4	3.2
1417184_s_at	Hbb-b1 /Hbb-b2	3.2
1438707_at	Atp13a4	3.2
1428776_at	Slc10a6	3.2
1417837_at	Phlda2	3.1
1450616_at	Ear5	3.1
1436058_at	Rsad2	3.1
1453092_at	Crct1	3.1

1420388_at	Prss12	3.0
1455527_at	Cd163l1	3.0
1448575_at	Il7r	3.0
1428988_at	Abcc3	3.0
1419043_a_at	Iigp1	3.0
1426960_a_at	Fa2h	3.0
1423494_at	2310042E22Rik	3.0
1429835_at	2310033E01Rik	3.0
1424357_at	Tmem45b	2.9
1418266_at	Alox12b	2.9
1440150_at	Tgm3	2.9
1460218_at	Cd52	2.9
1452257_at	Bdh1	2.9
1434465_x_at	Vldlr	2.9
1435748_at	Gda	2.9
1421370_a_at	Il1f5	2.9
1453055_at	Sema6d	2.8
1452614_at	Bcl2l15	2.8
1448299_at	Slc1a1	2.8
1435560_at	Itgal	2.8
1435111_at	2310011E23Rik	2.8
1418353_at	Cd5	2.8
1417141_at	Igtp	2.8
1416368_at	Gsta4	2.7
1454838_s_at	Pkdcc	2.7
1430697_at	Ammecr1	2.7
1452732_at	Asprv1	2.6
1433720_s_at	Chchd10	2.6
1422704_at	Gyk	2.6
1451756_at	Flt1	2.6
1439325_at	---	2.6
1422612_at	Hk2	2.6
1434382_at	Serinc2	2.6
1417094_at	Acot7	2.6
1455889_at	Far2	2.6
1417404_at	Elovl6	2.6
1416940_at	Ppif	2.6
1423634_at	Gsdma	2.6
1451594_s_at	Serpinb6c	2.5
1426734_at	Fam43a	2.5
1416592_at	Glrx	2.5
1417323_at	Psrc1	2.5
1417780_at	Lass4	2.5

1418181_at	Ptp4a3	2.5
1422784_at	Krt6a	2.5
1417956_at	Cidea	2.5
1419186_a_at	St8sia4	2.5
1415904_at	Lpl	2.4
1438531_at	A730054J21Rik	2.4
1434362_at	---	2.4
1429676_at	---	2.4
1437056_x_at	Crispld2	2.4
1423055_at	Nsg1	2.4
1428485_at	Car12	2.4
1418835_at	Phlda1	2.4
1416916_at	Elf3	2.4
1417932_at	Il18	2.4
1421930_at	Icos	2.4
1424011_at	Aqp9	2.3
1431554_a_at	Anxa9	2.3
1455048_at	Igsf3	2.3
1429567_at	Rassf10	2.3
1435695_a_at	Ggct	2.3
1427119_at	Spink4	2.3
1448617_at	Cd53	2.3
1424536_at	Oas1e	2.3
1416564_at	Sox7	2.3
1449279_at	Gpx2	2.3
1449265_at	Casp1	2.3
1450033_a_at	Stat1	2.3
1449959_x_at	Lce1h	2.2
1416022_at	Fabp5	2.2
1447541_s_at	Itgae	2.2
1422177_at	Il13ra2	2.2
1451895_a_at	Dhcr24	2.2
1427356_at	Fam89a	2.2
1434499_a_at	Ldhb	2.2
1435036_at	Aspg	2.2
1455106_a_at	Ckb	2.2
1423120_at	Ide	2.2
1419029_at	Ero1l	2.2
1418655_at	B4galnt1	2.2
1434873_a_at	Centb1	2.1
1451385_at	Fam162a	2.1
1423476_at	Slc46a2	2.1
1427221_at	Slc6a20a	2.1

1421923_at	Sh3bp5	2.1
1427052_at	Acacb	2.1
1424441_at	Slc27a4	2.1
1426243_at	Cth	2.1
1438658_a_at	S1pr3	2.1
1416383_a_at	Pcx	2.1
1460245_at	Klrd1	2.1
1435630_s_at	Acat2	2.1
1438961_s_at	Blmh	2.1
1416832_at	Slc39a8	2.1
1418930_at	Cxcl10	2.1
1449368_at	Dcn	2.1
1420503_at	Slc6a14	2.1
1424167_a_at	Pmm1	2.1
1460469_at	Tnfrsf9	2.1
1416318_at	Serpinb1a	2.1
1422478_a_at	Acss2	2.1
1436188_a_at	Ndrg4	2.1
1449591_at	Casp4	2.0
1421943_at	Tgfa	2.0
1424953_at	BC021614	2.0
1426440_at	Dhrs7	2.0
1457645_at	C130079G13Rik	2.0
1455049_at	Igsf3	2.0
1419738_a_at	Tpm2	2.0

Table S2.

Genes upregulated more than two-fold both in *RAC1*-null epidermis compared to control (n=4/4) and in 2d cultured *RAC1*-null keratinocytes from 3d old mice compared to control (n=3(pooled)/3(pooled)), identified by microarray gene expression analysis

Affymetrix ID	Gene name	2d cult in vitro	adult in vivo
1448756_at	S100a9	3.5	38.2
1419394_s_at	S100a8	3.8	32.0
1435639_at	2610528A11Rik	2.1	28.6
1426278_at	Ifi27l2a	2.1	23.1
1418580_at	Rtp4	5.2	16.0
1420771_at	Sprr2d	3.1	15.4
1419709_at	Stfa3	3.5	15.1
1422672_at	Sprr1b	5.3	13.2
1420550_at	Lce1f	7.1	12.4
1422240_s_at	Sprr2h	3.4	11.0
1427268_at	Flg	6.3	10.7
1424518_at	Apol9a/ Apol9b	4.9	10.6
1450783_at	Ifit1	4.3	9.0
1419215_at	Aox4	2.3	8.5
1420676_at	Lce1a1	4.3	8.4
1456539_at	---	3.8	8.4
1418609_at	Il1f6	2.0	7.0
1450618_a_at	Sprr2a	3.1	6.5
1424775_at	Oas1a	2.0	6.4
1435761_at	Stfa1	3.1	6.4
1435760_at	Csta	3.0	5.9
1422588_at	Krt6b	12.0	5.7
1448932_at	Krt16	3.2	5.7
1424921_at	Bst2	2.4	5.6
1431591_s_at	Isg15	4.6	5.3
1449938_at	Pp11r	2.6	5.3
1420332_x_at	Lce1d	3.3	4.9
1429862_at	Pla2g4e	3.3	4.7
1448380_at	Lgals3bp	2.5	4.7
1425715_at	Il1f8	3.7	4.5
1454159_a_at	Igfbp2	2.4	4.5
1429540_at	Cnfn	5.7	4.3

1448754_at	Rbp1	4.1	4.2
1448745_s_at	Lor	4.7	4.2
1418173_at	Krt25	2.1	4.1
1425958_at	Il1f9	6.9	4.0
1420741_x_at	Lce1i	3.2	4.0
1452592_at	Mgst2	2.0	3.8
1448982_at	Klk6	8.3	3.7
1451375_at	Ehf	3.0	3.6
1424549_at	Degs2	3.9	3.5
1449378_at	Krt27	2.1	3.4
1460603_at	Samd9l	2.0	3.4
1454264_at	2310046K23Rik	7.1	3.3
1438707_at	Atp13a4	5.0	3.2
1453092_at	Crct1	5.6	3.1
1423494_at	2310042E22Rik	4.5	3.0
1429835_at	2310033E01Rik	2.5	3.0
1418266_at	Alox12b	4.3	2.9
1421370_a_at	Il1f5	6.5	2.9
1435111_at	2310011E23Rik	4.1	2.8
1452732_at	Asprv1	5.7	2.6
1423634_at	Gsdma	4.7	2.6
1451594_s_at	Serpinb6c	2.0	2.5
1416592_at	Glrx	3.5	2.5
1417780_at	Lass4	2.2	2.5
1417956_at	Cidea	3.1	2.5
1429676_at	---	2.0	2.4
1450033_a_at	Stat1	3.2	2.3
1416022_at	Fabp5	5.4	2.2
1435036_at	Aspg	2.0	2.2
1416832_at	Slc39a8	2.6	2.1
1420503_at	Slc6a14	7.4	2.1
1416318_at	Serpinb1a	3.1	2.1
1436188_a_at	Ndrg4	2.6	2.1